University of Nevada, Reno

DEVELOPMENT OF A REDUCED-ORDER SIMULATION MODEL FOR THE NONLINEAR RESPONSE ANALYSIS OF A LARGE-SCALE LAMINAR SOIL BOX EXPERIMENTAL SYSTEM

A thesis submitted in partial fulfillment of the

Requirements for the degree of Master of Science in

Civil and Environmental Engineering

By

Pratibha Ghimire

Dr. Sherif Elfass/ Thesis Advisor

May 2024

THE GRADUATE SCHOOL

We recommend that the thesis
prepared under our supervision by

Pratibha Ghimire

entitled

Development of a Reduced-Order Simulation Model for the Nonlinear Response Analysis of a Large-Scale Laminar Soil Box Experimental System

be accepted in partial fulfillment of the
requirements for the degree of

Master of Science

Sherif Elfass, Ph.D.
Advisor

David McCallen, Ph.D.
Committee Member

John N. Louie, Ph.D.
Graduate School Representative

Markus Kemmelmeier, Ph.D., Dean
Graduate School

May, 2024

ABSTRACT

The stability of major structures is influenced by the properties of the soil on which the structure is founded. During earthquake shaking, soil deforms and transfers the vibrations to the supported structure. Consequently, the structure is displaced, and induced forces are transferred back into the soil through the foundation. These forces will affect the displacement of the soil, which will, in turn, modify the structure's vibration. This two-way relationship between soil and structure is referred to as Soil-Structure Interaction (SSI) and is not comprehensively addressed by most structural design codes. However, past earthquakes have demonstrated that SSI effects can influence structural damage. Critical infrastructures such as nuclear plants, large buildings, bridges, underground pipes, and tunnels are more vulnerable, and SSI should be considered for their design. A comprehensive understanding of SSI effects must be informed by observations of actual system performance. However, field installations of sensors along with their data acquisition systems to obtain detailed data on SSI during extreme events is challenging. To overcome this challenge, researchers have been using shake tables to conduct SSI tests. This type of tests provides a method for investigating the coupled soil and structure system using representative earthquake ground motions under carefully controlled conditions. Shake table testing can provide substantial data to analyze the soil and structure behavior in the laboratory, which can inform future design methodologies.

The University of Nevada, Reno, has recently developed a unique experimental capability by designing and commissioning the largest soil box in the nation along with its dedicated shake table. This experimental apparatus is capable of fully controlled large-scale experiments that can be used to study SSI in the laboratory under various soil conditions,

structure types, and ground motions. The study described herein focuses on developing a reduced-order computational model and comparing its output to the experimentally collected data for the same laminar soil box experiment. A 1-D soil column was developed in SAP2000. The compacted soil in the soil box was represented as a 1-D Timoshenko beam model. This model can provide an essential and efficient tool for capturing the response of the soil box. The model was developed to represent the nonlinear response behavior of the soil box system through continuous updating of the model shear modulus and damping ratios based on the effective strain of the soil. Through comparison with soil box response data from carefully controlled soil box system commissioning tests, the reduced order model was demonstrated to be capable of capturing the dynamic behavior of the overall soil box, including both low-amplitude linear vibrations and high-amplitude nonlinear response.

Acknowledgment

I feel privileged for the opportunity to be involved in soil box research at the University of Nevada, Reno. This journey would not be complete without the help of many individuals whom I want to thank from the bottom of my heart.

I sincerely thank my advisors, Dr. Sherif Elfass and Dr. David McCallen, for onboarding me on the research team and for continuous motivation, direction, and supervision throughout the academic journey. Similarly, I sincerely thank you for your support at every step of my research, from the beginning to the end.

Special thanks to Dr. Patrick Laplace, Chad Lyttle, and Todd Lyttle for their guidance and support during the experimental tasks. I appreciate my friends and family's immense help and support for being there for me whenever I need it the most. Also, I am grateful to my teachers, friends, and those countless memories I made at the University of Nevada, Reno, that I will cherish for my entire life.

My gratitude is incomplete without thanking Professor John Louie for accepting to be in my thesis committee and supporting me complete my graduate studies. Thank you for the helpful comments to refine my thesis document.

TABLE OF CONTENTS

LIST OF TABLES

LIST OF FIGURES

ABBREVIATIONS

Atm:	Atmospheric pressure
CSI:	Computers and Structures, Inc.
EB:	Elastomeric Bearing
E_o:	Initial Young's modulus
FSBM:	First order and Second moment Bayesian Method
Ft:	Feet
G:	Shear Modulus
G_{max}:	Maximum shear modulus
HSS:	Hollow Structural Steel
Hz:	Hertz
$K2_{max}$:	Shear modulus number
K_b:	Coefficient of lateral earth pressure at rest
Lb:	pound
LLSB:	Large-scale Laminar Soil Box
LRB:	Lead Rubber Bearings
MEMS:	Micro-Electro-Mechanical Systems
PGA:	Peak Ground Acceleration
SSI:	Soil-Structure-Interaction
PCF:	Pounds per cubic feet
PSF:	Pounds per square feet
ROM:	Reduced Order Model
SAP:	Structural Analysis Programming
υ:	Poisson's ratio
γ:	Unit weight
σ'_v:	Vertical effective stress
σ'_m:	Mean effective stress
ϕ:	Angle of internal friction

CHAPTER 1 INTRODUCTION

The substructure is an important component when determining the structural response during major earthquake events. Historically, structures were analyzed by assuming the superstructure to be a fixed base system with little to no attention to the effect of the substructure. As the structural response is dependent on the foundation soil, the study of the soil response becomes very important for the precise analysis of the structure. Laboratory shake table tests have been used for decades to study the soil response and its interaction with the structure during extreme events like earthquakes. The soil box experiment is time-demanding and expensive. The analytical model of the soil box would require computational power with large processing and storage capacity. A well-developed reduced order model using widely accepted structural analysis software would greatly impact this field by allowing reasonable prediction of SSI while conserving resources.

1.1 Earthquake response, including soil-structure-interaction

During an earthquake, the sudden movement of the earth's tectonic plates along the fault line releases stored strain energy, which propagates as seismic waves [1]. When seismic waves reach the earth's surface, strong shaking can damage infrastructures, causing a massive loss of property and life. These waves can generate tsunamis, seiche, liquefaction, landslides, retaining structures, or lifeline failures. The vibrations in the soil propagate to the structures lying above the crust and can result in significant structural damage or catastrophic failure. These structures have demonstrated failure in various modes, including gable wall failure, out-of-plane failure, in-plane failures, connection failures, delamination of walls, diaphragm failure, and mid-sectional vertical cracks on the masonry buildings, and failures associated with soft-story, and pancake failures in reinforced

concrete buildings. Physical structures providing shelter to many individuals are vulnerable to earthquakes. A modern construction approach can mitigate the loss of lives due to these failure modes by designing the structures to achieve proper earthquake-resistant design [2].

All the structures are constructed on geologic strata, typically consisting of a base soil. The soil supporting these structures can be loose/soft or dense/stiff depending on the geographical conditions. Different types of soil transfer seismic waves of various intensities based on the soil's density and other physical properties. As earthquakes create strong cyclic loading, this shaking can result in the nonlinear behavior of the soil. The natural composition of the soil is shaped by its origin, processes it went through, its porosity, and the stratified layers formed under the influence of the overlying soil pressure. Due to several factors like the heterogeneity of the soil composition, layout of the types of soils on the earth's surface, history of the formation of the landmarks, and moisture content in the soil in its natural form, generalization and mathematical representation of its nonlinearity can be complicated.

Structures and supporting soil are often analyzed in a decoupled fashion when studying their behavior during earthquakes. Seismic behavior is examined independently within geotechnical engineering to understand soil responses, whereas structural engineering focuses on analyzing the behavior of the overall structure. Both fields must interact together to understand the soil-structure behavior to ensure safe and reliable structural analysis. The interaction of the soil response during the earthquake with the structure and the impact of the structure on the soil are essential contributors to the system response. This interaction is known as soil structure interaction (SSI).

Buildings and bridges interact with the soil only in the basement or foundation zone. In the case of critical infrastructures like nuclear power plants and hydropower projects, many structures are built with substantial portions of the superstructure underground. Moreover, the same structure in different soil conditions may behave differently under the same earthquake. Consequently, soil-structure interaction is an area of interest, and controlled research is unavailable. In the case of these structures, several systems are connected to their corresponding components below the surface. Variations in their layout can result in high risk to life and property. Hence, a detailed analysis of the response of soil-structure interaction and the accuracy in computing the geotechnical parameters should be considered for designing such structures.

Even though the need to study soil-structure interaction in any critical structure is vital, validated methodologies for predicting the soil-structure interaction are very limited. Only a handful of methods are widely available. Direct and multistep are widely accepted methods for analyzing soil-structure interaction [2]. For the direct methods of soil-structure interaction analysis, a finite element model is prepared for an entire soil-foundation structure, with a free-field motion specified as an input motion, and a single-step analysis is carried out[2]. Multistep methods utilize superposition for the two different actions that happen simultaneously during the motion. They are kinematic interaction and inertial interaction. Kinematic interaction in the foundation occurs during ground motion, where the foundation moves due to the ground motion. As the foundation cannot sync with the free field motion, the effect of the structure on the soil is negligible in this interaction. Inertial interaction is the additional deformation in the soil caused by the transmission of

inertial forces of the foundation to the soil. This causes excessive soil displacement near the ground surface[3].

The methods discussed must be analyzed for representative soil conditions in several recorded ground motions. Codes and standards have been developed to analyze the structure's response based on site-specific parameters. A structure's location, proximity to the earthquake fault, and maximum probable earthquake intensity are utmost for critical infrastructure design. In addition, structure type, risk category, and other structural parameters govern the design. Though codes and standards for design practice cover most of these parameters, detailed site-specific studies should be carried out to design critical infrastructures safely.

For the appropriate designing of the system, natural frequency and mode shapes of the system are analyzed. Natural frequency of the system helps predict the frequency content of the system and the period at which it responds maximally to the ground motions. Natural mode shapes of the system predict the shape it deforms in while it is excited. This can be used to locate the weak spots of the system and help strengthen it. The acceleration response spectrum is also a vigorous tool that indicates the period range and the type of earthquake for which the system can be most vulnerable.

1.1.1 Natural frequency and natural mode shapes

A system experiences maximum acceleration when it is excited with a certain frequency. The frequency which resonates the system’s motion is known as its natural frequency. The natural frequency of a system characterizes its dynamic vibration as a function of stiffness and mass distribution. When the frequency content of earthquake ground motion matches

the structures' natural frequency, the structure can amplify the motion due to the occurred resonance. The Mexico City earthquake was one of the earthquakes where the resonance effect was clearly observed when the buildings of six to fifteen stories collapsed[4]. Developing reliable building codes and standards by carefully analyzing and categorizing the soil types can reduce such disasters by avoiding under-prediction of the design and confirming the earthquake resistance of the structures. When a stiff structure with higher natural frequency and lower fundamental period is built on hard soil type, the resonance of the wave can result in the amplification of the system response, causing high destruction of stiff structures. Similar amplification, resonance, and destruction could be expected when tall, flexible structures are constructed on loose soil. The response differs for the stiff structure constructed on loose soil and the flexible structure constructed on dense soil [5].

The unique deformed shapes observed when a system oscillates at its natural frequencies are its corresponding mode shapes. Each mode shape depends on the mass participating in constructing the unique shape. As the structure starts vibrating at a higher frequency, the mode shape simultaneously changes. In the fundamental frequency, the structure acquires a definite deflected shape known as the first mode shape, which is similar to the deformed shape obtained from a pushover analysis. The deflection pattern of a structure during any event is the combination of its mode shapes.

1.1.2 Acceleration response spectrum

A response spectrum is a pattern of oscillation peaks that emerges when a set of single-degree-of-freedom oscillators, each with varying frequency content, is introduced to a common vibrating base. Response spectrum can be created for displacement, velocity, and acceleration, but the research would primarily focus on the acceleration response spectrum

of the responses. The acceleration response spectrum of a ground motion describes the earthquake pattern and has been widely used to assess the earthquake's impact on the structure [6]. If the peak of the acceleration response spectrum of any earthquake is observed at a short period, the earthquake would have the potential to amplify the response of the short-period structures, resulting in resonance with that structure, and vice versa. Hence, the response spectrum is a robust tool for predicting significant seismic damages, and its consideration during design creates a safe and reliable infrastructure.

The composition of the soil layers alters the response pattern due to the propagation velocity of shear waves in the two adjacent layers. Soft soil has lower shear wave velocity with lower frequency content than dense soil. This results in a further extended natural period of vibration in loose soil when the acceleration response spectrums of loose and dense soils are compared [7].

1.2 Attributes and function of the UNR laminar soil box system

Numerous approaches have been used when investigating the seismic response of soil. One of the most applicable approaches is through conducting large-scale experiments utilizing a large soil box and subjecting it to earthquake ground motions. Experimental tests and comparative analyses have been conducted to study the soil behavior using a soil box mounted on shake tables [5]. However, the scope of these studies may have been restricted by the considerable technical and financial hurdles associated with developing a large soil box capable of accurately replicating infinite soil behavior during seismic events. Ideally, a soil box is designed to retain the soil without constraining it. Soil is compacted inside the box, which is then positioned atop a low-friction platform referred to as the shake table platen. This shake table is responsible for generating realistic earthquake ground motions.

These ground motions propagate through the soil and reach the top of the box. An experiment involving a soil box on a shake table serves to emulate soil-structure interaction under conditions that closely mirror real-world field scenarios.

Shake-table tests have been carried out at several universities. The test in the State Key Laboratory on Disaster Reduction in Civil Engineering at the Tongji University of China concluded that soft soil could filter and isolate vibration[9]. With the increase in input acceleration, the amplification factors of acceleration peak values can be reduced due to the non-linearity of the soil[10].

The analysis carried out at Lotung in Taiwan obtained insight regarding the validity of the soil structure interaction, namely, that vertical wave propagation assumption describes the wave field and equivalent linear analysis provides a significant but temporary degradation of soil modulus. It was also noted that developing soil stiffness degradation and damping curves as a function of strain requires improvement to reduce variability and uncertainty[8]. From the soil collected at several locations, the plots of the shear modulus reduction and damping ratios with varying strain for various confinement pressure were obtained. These curves are referred for the development of this reduced order model.

As per the research for the design of large-scale biaxial laminar soil box (LLSB) for seismic soil structure interaction studies carried out at the University of Nevada Reno, a simulation model was created to assess the dynamic response of a 1D soil column followed by a 2D slice to include the proposed wall of the soil box and a 3D model [11]. A 3D model of the soil box was generated for more accurate assessment of the expected performance of the soil box. It was observed that the response at low amplitude accelerations of the peak ground acceleration (PGA) of up to 0.5g, the responses were essentially linear and

comparable for both equivalent linear and nonlinear analysis methods. When high amplitude ground motions with the PGA of more than 0.5g were introduced in the model, high variations were observed between the responses from equivalent linear and nonlinear methods, indicating system's nonlinear response [11]. This observed nonlinearity limited the increase of base shear and increased soil strains significantly, resulting in de-amplification of input motion towards the surface. In this case, the linear model overpredicted the base shear forces and underpredicted the shear strain for higher amplitude shaking. Due to the sizeable overturning moment generated at the bottom of the soil box while analyzing the significant ground motion, the wall of the soil box had to be designed to ensure support for both transverse shear and tension. Walls and connections had to be designed with minor lateral stiffness and very high axial and bending stiffness[11]. Based on an extensive simulation-based study, risk-mitigation experiments, and extensive experience, a large-scale biaxial laminar soil box (shown in Figure 1) was successfully designed, built, and commissioned at the University of Nevada, Reno, to study seismic soil-structural interaction [11].

Figure 1: Soil box built at the University of Nevada, Reno

Once the box was built, it was shaken while empty to determine its dynamic performance and compare it with the design criteria and numerical models. Following this experiment, the box was filled with densely compacted soil and subsequently exposed to a diverse array of ground motions featuring varying amplitudes. Given the importance of having a predictive model for representing the observed behavior in designing future experiments, developing a reduced-order model will provide an essential tool for providing information on the parameters influencing soil-structure interaction and predicting the response to be expected during the experiment.

1.3 Objectives of the current study

This study emphasizes developing a reduced order model using readily available structural analysis software. The model can be used for predicting the behavior of the soil box system during an experiment. The objectives of this study include:

- To develop a reduced order numerical model of the soil column of the soil box to capture the linear and nonlinear responses using readily available finite element analysis software.
- To analyze the frequency and mode shapes of the analytical model and compare them to the experimental results.
- To study the acceleration response spectrum of the acceleration recorded at the top of the soil box with compacted soil and compare it with the reduced order model.
- To compare the time history of the acceleration responses recorded from the soil with the ground motion to the simulation model.

CHAPTER 2 COMMISSIONING OF THE SOIL BOX AND EXPERIMENTAL BOX RESPONSE

The octagonal soil box, mounted on the shake table at the University of Nevada, Reno, was designed to investigate the soil's complex behavior and interaction with a structure during simulated earthquake events. The commissioning of the soil box includes the initial assembly of the box, its placement on the shake table, the shake table experiments with an empty soil box, the compaction of the soil in the soil box, and the final dynamic testing, including soil in the box.

2.1 Design and assembly of the soil box

For a successful design of a soil box, the soil must be the one dominating the response of the soil box/soil system. In other words, the box must be designed such that it does not affect the response of the soil. As a result, the box included components like elastomeric bearings and steel beams to achieve this objective. The elastomeric bearings provide the necessary stiffness to deform with the soil without constraining it, while the steel beams provide the mass to form a coupled system. Such a system allowed the soil to behave independently from the box during and post shaking.

2.1.1 Elastomeric Bearings

Lead rubber bearings (LRB) are typically used to decouple the ground and the superstructure, thus isolating the superstructure from earthquake damage. The UNR laminar shear soil box system employed elastomeric bearings, which are similar to LRB but without the lead core. These elastomeric bearings were used to allow the soil box system to achieve a global shear deformation response when subjected to base shaking to emulate soil response in the field. In-situ soil has the behavior of transmitting seismic

waves based on shear-dominated movement.

Figure 2: Elastomeric bearing on soil box

Elastomeric bearings possess significant compressive stiffness but low tensile stiffness. They are also flexible in shear, thus providing the global shear-dominated behavior of the box. A total of 408 bearings were designed, tested, and attached in the soil box to the steel frames, as seen in Figure 2. The size, number, and arrangement of the bearings can be seen in Figure 3 [11].

Depth	Number Bearing	Type of Bearing	Type	Size of Bearing
0	8	RB1	A	8″
	8	RB1	A	8″
	8	RB1	A	8″
	8	RB2	B	11″
	8	RB2	B	11″
	16	RB2	B	11″
	16	RB2	B	11″
5	16	RB2	B	11″
	16	RB3	C	11″
	16	RB3	C	11″
	32	RB3	C	11″
	32	RB3	C	11″
	32	RB3	C	11″
10	32	RB3	C	11″
	32	RB4	D	11″
	32	RB4	D	11″
	32	RB4	D	11″
	32	RB4	D	11″
	32	RB5	E	11″
15	408			

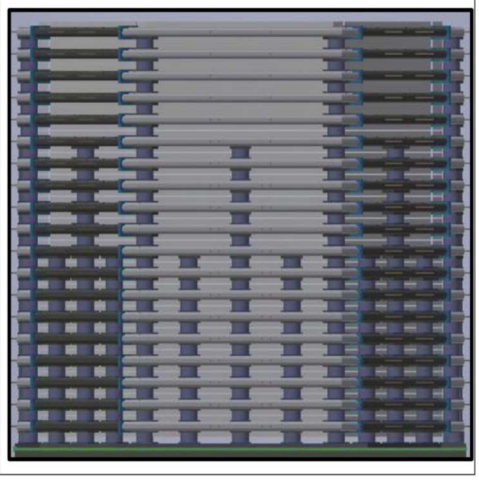

Figure 3: Size and arrangement of elastomeric bearings

This distribution of the elastomeric bearings ensures that the lower section of the soil box profile stays stiffer compared to the upper layers, matching the increase in soil shear stiffness at depth. The properties of the five types of elastomeric bearings were verified through a rigorous test program. They were categorized based on their stiffness and were arranged in the soil box, with mechanical properties listed in Table 1[12].

Table 1: Properties of elastomeric bearings

EB Outer Dia.	Bearing Type / Disp.	Effective Shear Stiffness (U2, U3) For displacement of:			Stiffness		K tor (R1)	K lin (R2)
					Compressive (A1)	Tensile (A2)		
		100%	25%	7%	k/in	k/in	k-in/ rad	k-in/ rad
8	RB1	1.13	1.21	1.42	224	170	2.32	252
11	RB2	2.76	3.36	3.7	890	757	4.99	2485
11	RB3	4.73	5.62	6.77	1541	1154	9.59	4777
11	RB4	8.35	10.11	12.88	2020	1679	16.9	8414
11	RB5	10.81	13.08	16.65	3525	2931	21.89	10899

2.1.2 Steel section

The steel sections for the soil box were selected as rectangular hollow structural steel (HSS) sections (tubes), as observed in Figure 4. While all tubes have the same outer dimensions (14x4 inches), two tube thicknesses, representing two different weights per unit length, were used. The heavy sections were used in the lower five (5) frames, while the rest used the lighter sections. A faceplate was welded to the tubes to retain the soil inside the box. These adjacent layers were assembled with elastomeric bearings by attaching them to the rectangular portion of the steel frame. The assembled soil box consists of 19 layers of HSS sections, 19 layers of elastomeric bearings, and a 2-inch-thick base plate holding

it. The section was prepared such that its final assembly would result in a regular octagonal box, as shown in Figure 5. The shape of the soil box was selected to be octagonal for the ease of guiding the box in case of uniaxial shaking. This feature, however, requires a guiding frame which was not fabricated as part of this effort [9]. The stiffness of the layers was maintained to divide the soil box stiffness into three different segments of 5 feet each. This functions as a three-storied structure with the highest stiffness at the bottom and the lowest at the top. The segments were bolted individually with the definite elastomeric bearings numbered according to the size and stiffness. More information about the design of the box can be found in the research about design, fabrication, and commissioning of this soil box [13].]

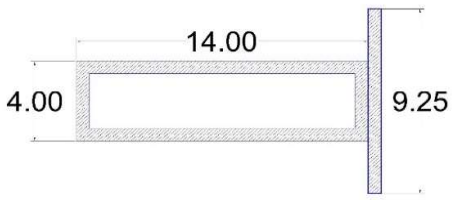

Figure 4: HSS section of the box

Figure 5: Picture of the assembled soil box in the laboratory

2.1.3 Shake Table

A shake table is constructed to transfer the targeted ground motion to the soil box system. It consists of several components, among which is the table platform at the top of the shaking table, which is a base for the testing structure. It is classified by its method of

vibration actuation as electrically, hydraulically, and manually driven [14]. Also, it can be classified based on the direction of the movement: uniaxial table with motion in one horizontal direction, biaxial table with two horizontal directions, and triaxial table in three orthogonal directions. The selection of the shake table is based on the requirements of the experiment.

The large-scale laminar soil box shake table was designed as a biaxial table that imparts two horizontal motion components. The shake table was prepared with high precision to create earthquake motions while supporting a large vertical load from the supported soil mass. The shake table was designed to hold approximately 400 tons of compacted soil and box weight in combination. In Figure 6, hydraulic bearings supporting the intended shake table location can be observed.

Figure 6: Positioning of the shake table

For the placement of the shake table, once the location was finalized, the shake table elements were mounted on the hydraulic bearings, as indicated in Figure 7. The actuators and valves were assembled, and the control system was set up to impose the desired earthquake motion accurately. The shake table was designed to have very low friction so that the hydraulic actuators could readily generate the desired earthquake motions.

Hydraulic actuators, indicated in Figure 8, which act as a piston, are used to generate controlled vibration to the shake table. These actuators were arranged in such an orientation that they could induce the desired bi-axial ground motion in two horizontal directions. As shown in Figure 9, the attached platform transmitted the induced target ground motion directly to the soil box.

Figure 7: Shake table assembly

Figure 8: Hydraulic actuators

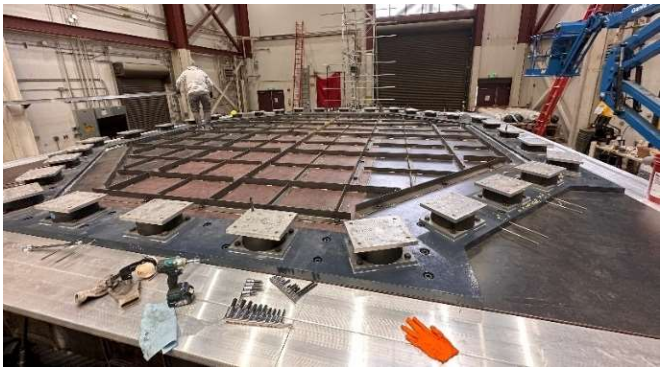

Figure 9: Soil box base platform attached to shake table

2.2 Fabrication and construction

The fabrication and commissioning of the soil box includes the preparation of the soil box for compacting the soil and arranging for the shake table test.

2.2.1 Soil box

The soil box creates the environment for soil confinement and represents the characteristic soil behavior during earthquake shaking. The steel structure has a rectangular section attached to the plate to retain the soil inside the box. The stiffness of the soil increases as the depth increases due to the overburden pressure in its natural condition, which is replicated in this experimental setup by the distribution of the bearings as seen in Figure 10. Due to lower stiffness, the upper portion of the soil will have higher displacement.

Figure 10: Soil box in the Laboratory used for experiment

Fewer numbers of elastomeric bearings were used in the upper layer in order not to impede soil deformation. The empty box was commissioned at its full height of 15 ft. Once the empty soil box was commissioned and tested, the next phase of commissioning included evaluating the system response with soil inside the box. Due to schedule and financial constraints, as well as the negligible impact on commissioning results, the box was filled with compacted soil up to a height of 10 ft only. Thus, the lower five (5) feet of the soil box was removed, and the upper two segments (representing 10 ft) were mounted onto the shake table for this commissioning activity. The segments used for the experiment are shown in Figure 11 as the segments connected to the crane in preparation of the test setup. The height of the compacted soil in this portion of the box was 120 inches.

Figure 11: Soil box portion used for further analysis

2.2.2 Sealing the gap between faceplates

The soil box layers were separated into five-foot segments for workability. To stop the soil from spilling out of the box during compaction and testing, silicone tubes were used to seal the gap between the faceplates, as shown in Figure 12. The gap between the bottom frame and the base plate was sealed using a plastic sheet by loosely attaching it to the steel plate using duct tape, as demonstrated in Figure 13. The sealing materials were selected to stay flexible enough to avoid soil scattering out of the box without exerting additional pressure on the soil and not altering the movement pattern.

Figure 12: Silicone tube sealing the gap

Figure 13: Plastic sheets sealing the gap

2.2.3 Mounting the soil box on the shake table

The box segments were bolted separately and were hauled from the assembly area onto the shake table. A double girder crane system in the laboratory, as shown in Figure 14, moved the box segments over the table using a steel beam.

Figure 14: Hauling of soil box segment using double girder crane

2.2.4 Soil compaction

The soil used in the experiment was transported from a local pit and stored in the laboratory's fabrication yard, as shown in Figure 15. The mechanical properties of the soil were assessed through index and soil strength tests. For deposition, the soil was loaded into a hopper using a front-end loader.

Figure 15: Soil stored in the fabrication yard

Figure 16: Forklift hauling the soil hopper to the lab

The hopper was then transported to inside the lab where the box resides using a large forklift, as shown in Figure 16. Figure 17 shows the hopper filled with soil placed inside

the laboratory, ready to be hauled to the soil box. Using the overhead crane, the soil-filled hopper was raised above the soil box, as shown in Figure 18, and the soil was deposited in it, as in Figure 19. A load cell, mounted onto the crane, was employed to determine the weight of each load from the hopper. This value was then utilized to calculate the density of each lift after measuring its height. The weight of the soil contained by the hopper during each lift was approximately 9,000 lb.

Figure 17: Hopper full of soil ready to be lifted

Figure 18: Hopper pouring soil in the box

Figure 19: Using hopper to pour soil

Shovels, tampers, rakes, and other leveling tools were used to evenly distribute the soil, as seen in Figure 20. A vibratory plate compactor was used to compact the soil. A hand tamper was used in areas where the compactor could not easily reach. Water was occasionally sprinkled to help increase the compaction of the soil, as in Figure 21. The vibratory plate compactor was used for three passes after each hopper deposit to ensure adequate compaction. Following every three consecutive compactions, a laser level was used to measure the elevation of the compacted layer at various locations in a grid pattern, as seen in Figure 22. To ensure appropriate compaction, the depth of each layer was targeted to be a maximum of three inches. The same steps were repeated until the final level of soil deposit was achieved.

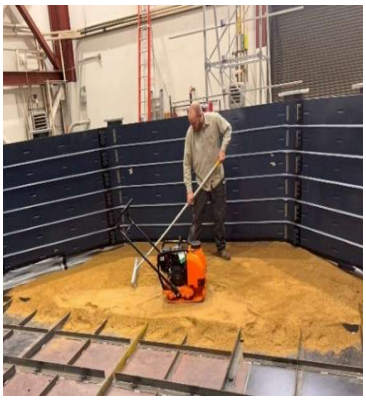

Figure 20: Leveling the soil

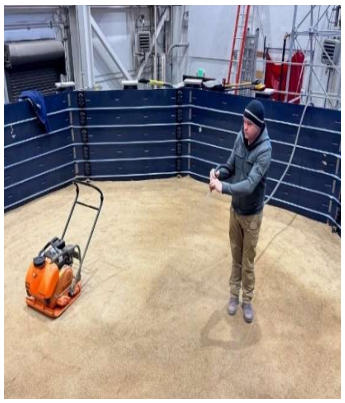

Figure 21: Sprinkling water for compaction

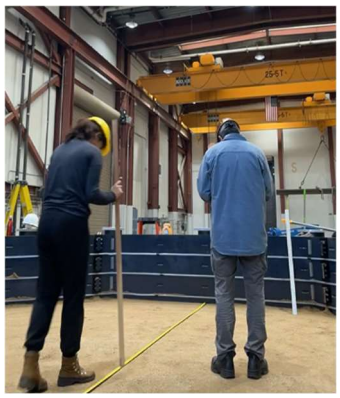

Figure 22: Measuring the level of compacted soil

2.3 Experimentally observed response of the soil box system

The soil box was subjected to several earthquake ground motions, and the acceleration at different levels within the soil mass including the top of the soil was recorded. The shake table induced 32 strong ground motions to the soil box with compacted sandy soil. The motions used for the experiment are listed in Table 2. It is noted that the earthquake motions were normalized to 1g acceleration at 100% amplitude. These motions were selected to drive the soil from the linear to the nonlinear range at higher amplitudes. Both linear and nonlinear responses of the soil were all recorded during all excitations. The responses from these experiments are used to validate the reduced order model in this research. The ground motions selected for the validation of the reduced order model were normalized motions for El Centro 1964 earthquake at 10% and 80% amplitude in the X-axis only. Figure 23 presents an image of the soil box, and the vertical red line indicates the initial resting position of the soil box before the commencement of the test. The installed sensors recorded the soil response during ground shaking.

Table 2: Ground motions induced in soil box with soil

Load	Description	Direction	Peak Acceleration (g)	Notes
1	White Noise	X	RMS = 0.0065g (1-20 Hz)	
2	White Noise	Y	RMS = 0.0065g (1-20 Hz)	
3	El Centro	X	5%	
4	El Centro	Y	5%	
5	El Centro	X + Y	5%	
6	El Centro	X	10%	
7	El Centro	Y	10%	
8	El Centro	X + Y	10%	
9	White Noise	X	RMS = 0.05g (1-20 Hz)	
10	White Noise	Y	RMS = 0.05g (1-20 Hz)	
11	El Centro	X	10%	4 channels added
12	El Centro	Y	10%	
13	El Centro	X + Y	10%	
14	El Centro	X	15%	
15	El Centro	Y	15%	
16	El Centro	X + Y	15%	
17	El Centro	X	25%	
18	El Centro	Y	25%	
19	El Centro	X	50%	
20	El Centro	Y	50%	
21	White Noise	X	RMS = 0.05g (1-20 Hz)	
22	White Noise	Y	RMS = 0.05g (1-20 Hz)	
23	El Centro	X	50%	
24	El Centro	Y	50%	
25	El Centro	X	60%	
26	El Centro	Y	60%	
27	El Centro	X	70%	
29	El Centro	Y	70%	Last motion repeat
30	White Noise	X	RMS = 0.05g (1-20 Hz)	
31	White Noise	Y	RMS = 0.05g (1-20 Hz)	
33	Cerro	X + Y	0.25g	9:35 AM
34	White Noise	X		System ID
35	White Noise	Y		System ID
36	Sine Wave	X		8 Hz
37	Sine Wave	Y		8 Hz
38	White Noise	X		System ID
39	El Centro	X	80% (0.8 g)	Achieved 0.98g
40	White Noise	X	RMS = 0.1g (1-20 Hz)	

Figure 23: Soil box deflection due to ground motion

2.4 Instrumentation

Several instruments and sensors were used to record the displacement and acceleration of the soil box. Instruments like string pots, Novotechnik and surface accelerometers were used on the empty soil box. During the experiment with compacted soil, embedded accelerometers and soil pressure cells were used.

2.4.1 Instruments used on the empty soil box

The empty soil box was fitted with sensors to record the acceleration and displacement response when subjected to ground shaking. This response data was recorded to serve as a benchmark for box performance when comparing it with the response of box with soil. Five triaxial accelerometers were placed on the outer side of the box wall to measure the acceleration in X, Y, Z directions.

String pots mounted onto a fixed reference frame placed off the shake table were used to record absolute displacements at various locations of the box wall. String pots are sensors with thin retractable strings with one end attached to the moving system and the other

attached to the stationary surface, as shown in Figure 24 and Figure 25. Linear position sensors (LPS, called Novotechnik) were placed between the box frames to measure relative displacement between the box frames, as indicated in Figure 26. LPS are sensors that convert the mechanical motion to an electrical signal [13] and record it.

Figure 24: Stringpot fixed to the stationary surface

Figure 25: Stringpots attached to the soil box

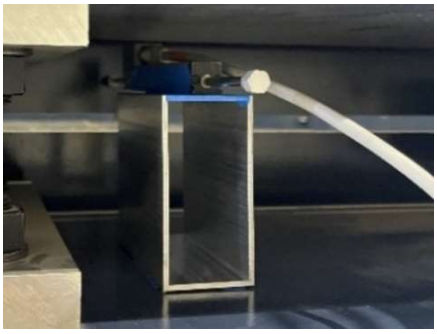

Figure 26: Novotechnik used in Soil Box

2.4.2 Sensors embedded in the compacted soil

Triaxial MEMS accelerometers were embedded in the soil mass at different depths, as shown in Figure 27. They were used to record the acceleration at these points within the soil mass. During the compaction of the soil, three accelerometers were embedded every 15 inches of height. This resulted in eight (8) levels of embedded accelerometers. The accelerometers were placed in three vertical arrays, one is at the center of the soil box, one close to the edge of the soil box, and one in mid distance between the previous two arrays. All the accelerometers were capable of recording three directional components of acceleration. The responses of the accelerometers embedded at the center of the soil box were analyzed. The acceleration response spectrum of the experimental setup was compared to the simulation model to develop the reduced order model. The levels of

location of the accelerometers and the procedure of installing the accelerometers are indicated in Figures 27 to 29.

Figure 27: Installation of embedded accelerometers

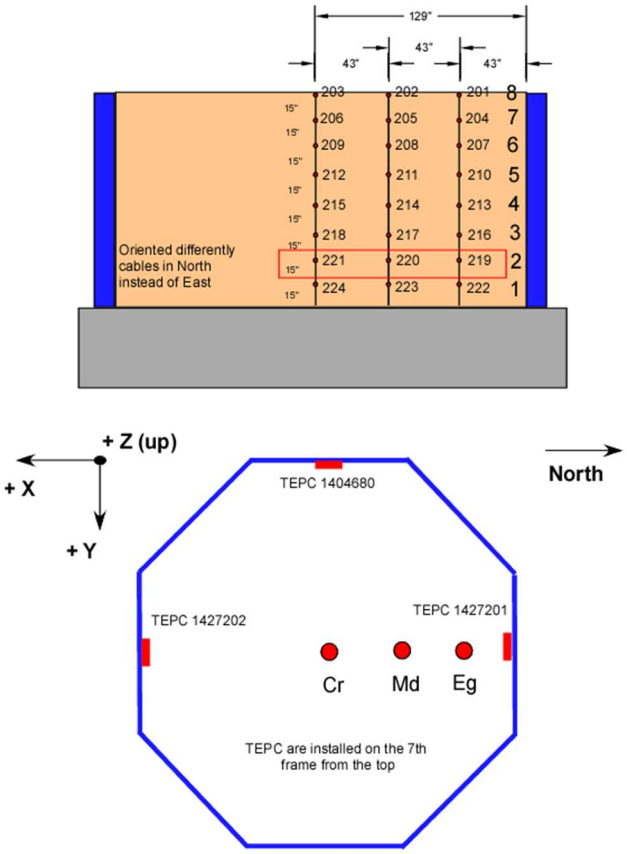

Figure 28: Level and location of embedded accelerometers

Figure 29: Positioning of embedded accelerometer

In addition to the embedded accelerometers, three total earth pressure cells were installed in three directions – North, South, and West. These sensors were used to capture the pressure exerted by the soil on the soil box wall. If the exerted pressure became negative, it indicated that the soil has formed a gap with the soil box wall during the motion, and the

following pulse of motion will cause sudden pounding, resulting in high impulse. As the soil softens, a rise in the pressure exerted would be expected. The installation of the pressure cells inside the soil box is indicated in Figure 30.

Continuous monitoring and evaluation were carried out during the whole procedure to ensure the proper safety of the soil box and work procedure. Figure 31 indicates the monitoring procedure from inside the laboratory.

Figure 30: Earth pressure cell

Figure 31: Monitoring the work and safety issues

2.5 Responses of empty soil box

After the empty soil box was shaken with the ground motions, the natural frequency and the mode shapes were derived from the results and the responses were analyzed. As the empty soil box was not simulated, the study of the empty soil box are solely based on the experimental results.

2.5.1 Natural frequency of empty soil box

The natural frequency of the empty soil box was analyzed. For the analytical study of the experimental model, the soil box was divided into three sections of five feet each - A, B, and C, as shown in Figure 32. The accelerometers at the surface of the empty soil box were placed at four different levels, at bottom of layer A, interface of AB, interface of BC, and

at the top of C, at the heights of 4.5 inches, 63 inches, 121.5 inches, and 180 inches, from the base respectively.

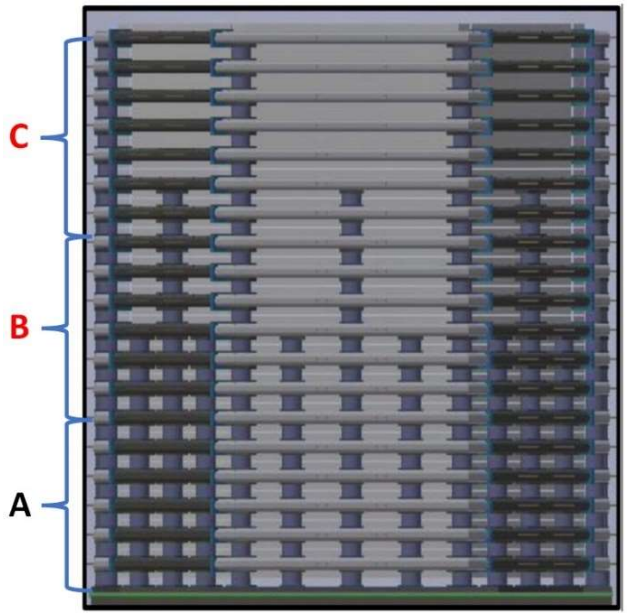

Figure 32: Soil box segmented for analytical study.

The frequency response function of the accelerations recorded by these accelerometers was calculated with reference to the plate accelerometer to study the frequency content of the soil box, as plotted in Figure 33. The four consecutive natural frequencies of the soil box observed were 1.88 Hz, 4.00 Hz, 6.50 Hz, and 8.63 Hz.

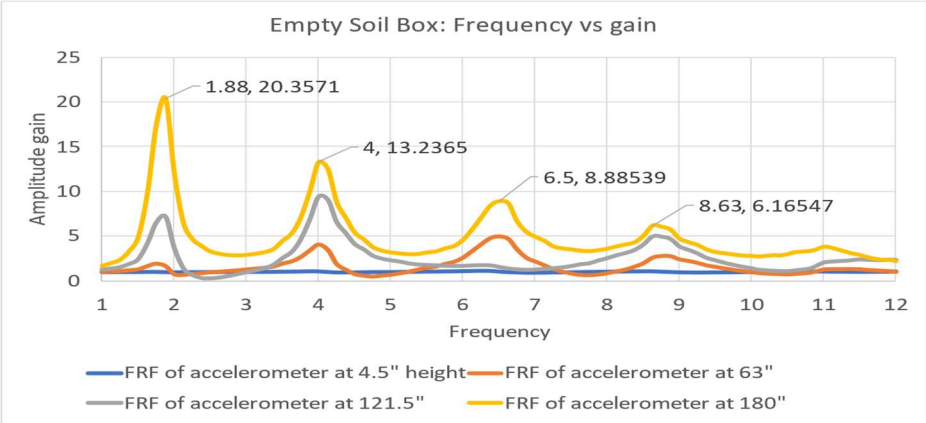

Figure 33: Consecutive natural frequency of empty soil box

The frequency content and amplitude gain of the experimental model with respect to varying intensities of ground motion are listed in Table 3. The first four modes were captured within the frequency of 12 Hz.

Table 3: Frequencies recorded from the dynamic test of the soil box

0.05g White Noise			Gain	freq1	Gain	freq2	Gain	freq3	Gain	freq4
X-Axis	25%	@ 25%	1.09	**1.97**	1.09	**4.21**	1.07	**6.73**	1.06	**9.35**
	50%	@ 50%	1.96	**1.91**	4.06	**4.18**	4.95	**6.69**	2.78	**9.19**
	75%	@ 75%	7.20	**1.87**	9.44	**4.14**	1.77	**6.69**	5.01	**8.87**
	100%	@ 100%	20.35	**1.88**	13.24	**4.04**	8.89	**6.51**	6.17	**8.63**
Y-Axis	25%	@ 25%	1.02	**1.91**	1.01	**4.18**	1.01	**6.66**	1.00	**9.4**
	50%	@ 50%	1.92	**1.86**	3.88	**4.07**	5.23	**6.67**	2.88	**8.78**
	75%	@ 75%	6.95	**1.83**	9.28	**4.08**	9.33	**6.52**	4.99	**9.16**
	100%	@ 100%	19.74	**1.82**	12.84	**4**	1.63	**6.5**	6.22	**8.7**

2.5.2 Natural mode shapes of empty soil box

Displacement of the empty soil box recorded during the low-intensity sine sweep ground motion was analyzed to acquire its mode shapes. The sine sweep is a sinusoidal ground motion with a collection of varying frequencies. In Figure 34, it can be observed that at a certain frequency of the sine sweep motion, the soil box amplifies its acceleration. These peaks of the acceleration at the top of the soil box would indicate the exact point of time at which maximum frequency content was observed.

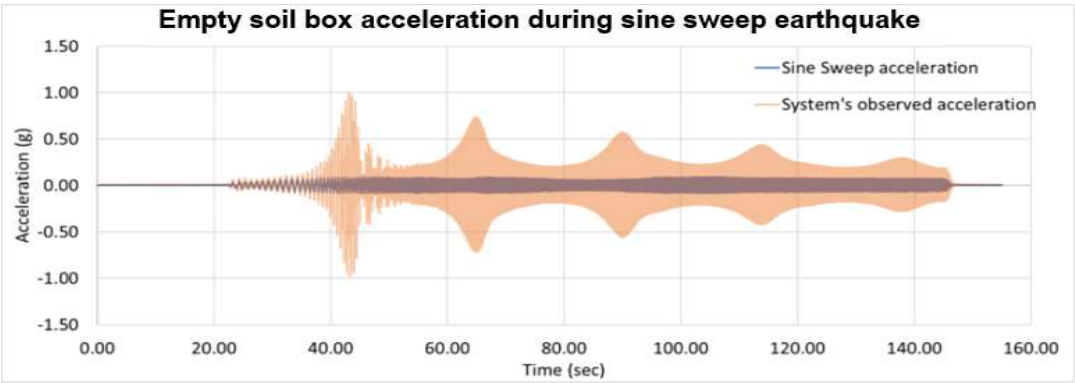

Figure 34: Time history of soil box excited with sine sweep ground motion

Using the recorded data from the string pots at several locations of the soil box, the displacement at each level during several frequency peaks was obtained. The fundamental and second frequency peaks are plotted in Figure 35 and Figure 36.

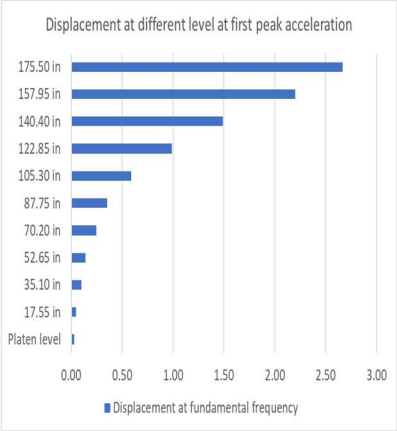

Figure 35: Displacement of empty soil box at fundamental frequency peak

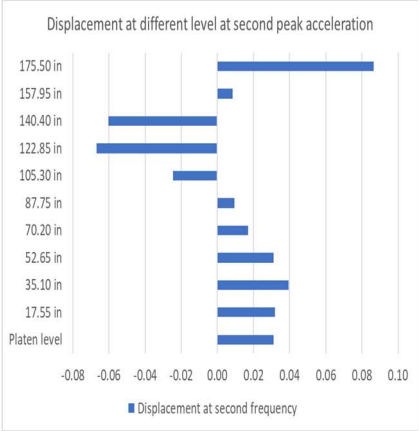

Figure 36: Displacement of empty soil box at a second frequency peak

The mode shape of the soil box was obtained by converting the deformations to unit maximum displacement. As four frequency peaks were distinct during the experiment, four distinct mode shapes were obtained. The mode shapes of the empty soil box can be observed in Figures 37-40.

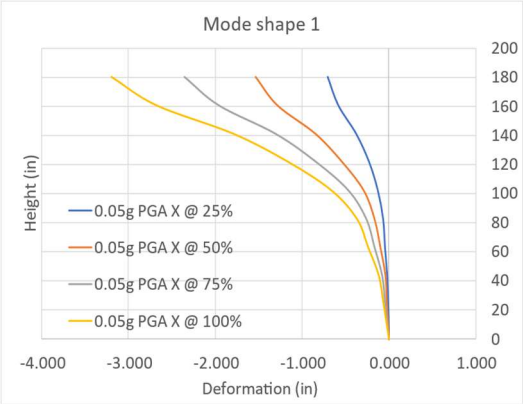

Figure 37: Empty box mode shape 1

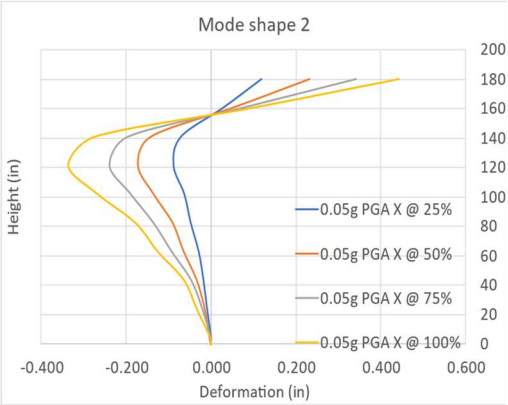

Figure 38: Empty box mode shape 2

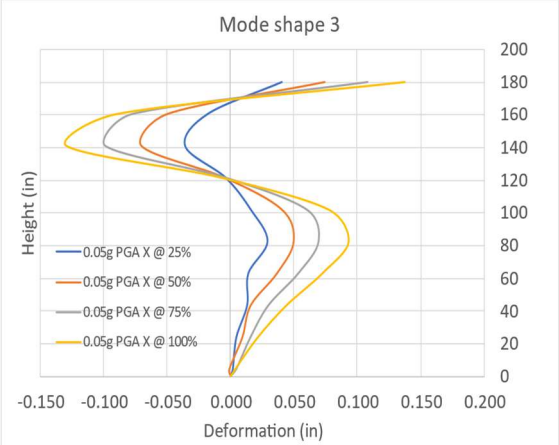

Figure 39: Empty box mode shape 3

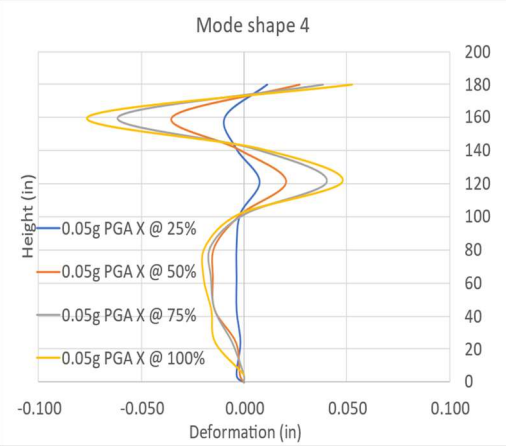

Figure 40: Empty box mode shape 4

The mode shapes of the empty soil box align with the mode shapes of the Euler-Bernoulli beam[15]. The fundamental mode shape was observed when the soil box attained a frequency of 1.88 Hz. As the box oscillated at 4.00 Hz, 6.50 Hz, and 8.63 Hz, mode shapes 2, 3, and 4 were simultaneously observed.

2.6 Responses of soil box with soil

Based on the results of the ground motions for the soil box with compacted soil, the natural frequency and the mode shapes of the box were derived. The responses are compared to

that of the empty soil box to understand the soil behavior. These derived responses would be compared to the responses obtained from the reduced order model.

2.6.1 Natural frequency of the box with compacted soil

The fundamental frequency of the soil box filled with compacted soil during the laboratory test was obtained by applying Fourier transformation to the response of the embedded accelerometers. As expected, significant differences were observed compared to the natural frequency of the empty box. Figure 41 represents the frequency and amplitude gain of the soil box with compacted soil at several levels before the soil yielded.

As the intensity of the ground motions increased, the soil ultimately yielded. This became apparent as the soil underwent a shear strain of 2%. The frequency of the soil box with soil was reduced significantly as the soil softened due to the yielding, as observed in Figure 42.

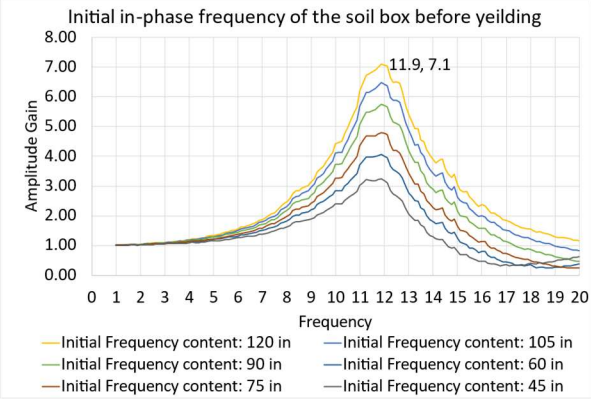

Figure 41: Frequency of soil box with soil before yielding

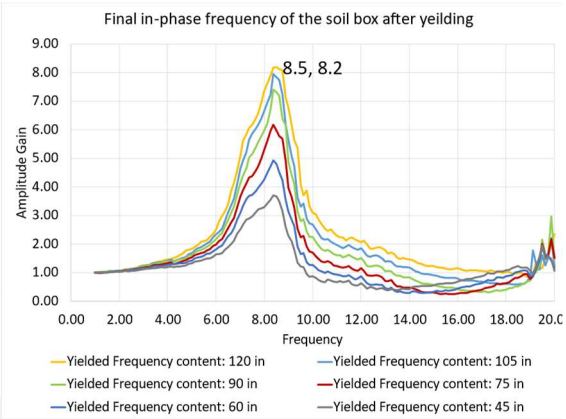

Figure 42: Frequency of soil box with soil after yielding

The fundamental frequency of the soil box calculated using the acceleration recorded by embedded accelerometers during several earthquake motions is tabulated in Table 4. It can be observed from the table that the frequency of the soil box with compacted soil at the initial condition of 11.9 Hz decreased to 8.5 Hz when the soil yielded due to high-intensity

ground motions. The soil-filled box underwent sinusoidal motion right after motion 35. The sine wave, resonating at the soil's natural frequency of 8 Hz, caused compaction of the soil and subsequent stiffening of it. This transformation was evident by the increase in natural frequency observed during motion 38.

Table 4: Natural frequency of embedded accelerometers at the top of the soil

Eq.	Ground Motions	Average frequency (Hz)			
SN.		X-box	X-Soil	Y-box	Y-Soil
1,2	White Noise 0.05g RMS @ 13%	11.95	11.90	11.75	11.60
,9,10	White Noise 0.05g peak 1-20 Hz	11.55	11.20	11.15	11.10
21,22	White Noise 0.05g peak 1-20 Hz	10.85	10.50	10.00	10.00
30,31	White Noise 0.05g peak 1-20 Hz	9.20	9.20	8.20	8.20
34,35	White Noise System ID	8.50	7.83	7.40	7.40
38	White Noise System ID	9.90	9.60	-	-
40	White Noise 0.05g peak 1-20 Hz @ 200%	8.70	8.20	-	-

2.6.2 Natural mode shapes of soil box with compacted soil

As sine sweep was not introduced for the experiment of the box filled with soil, the mode shapes could not be directly obtained from displacement recorded during the experiment. The mode shape was obtained by plotting the maximum amplitude gain of the frequency at varying heights, assuming maximum unit deformation. The fundamental mode shape of the soil box with soil seen in Figure 43 is equivalent to the mode shape of a shear beam [15]. No other mode shapes could be obtained from the experiment as the soil box experiment was carried out to capture frequencies up to 20 Hz. The amplitude gain of the

soil box with compacted soil at the fundamental frequency with varying heights of accelerometers placed was plotted. The maximum amplitude gain was unitized, as observed in Figure 43. The amplitude gains of the soil box with compacted soil at each level at unyielded conditions and after yielding had a similar ratio. The mode shape of the soil box at unyielded conditions would hence be the same as the mode shape of the soil box after yielding. At both conditions, the second frequency peak was not observed.

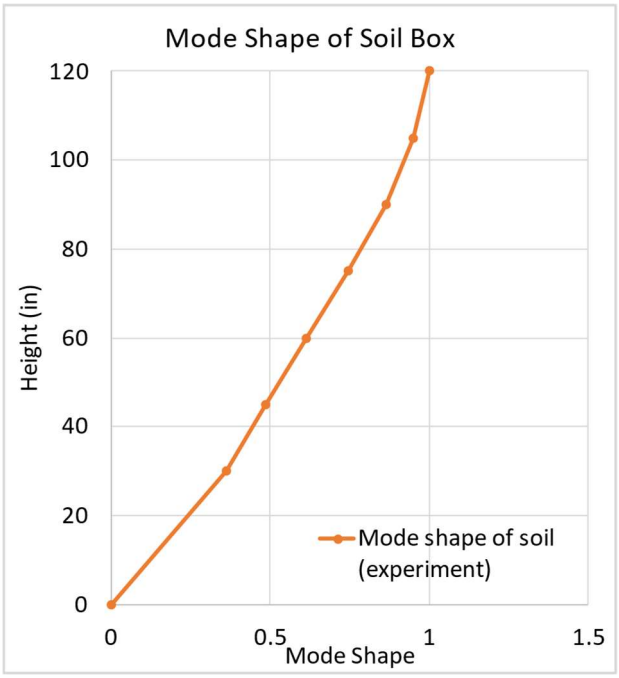

Figure 43: Mode shape of soil box with soil from experiment

2.6.3 Acceleration response due to earthquake excitation

For the further analysis and development of the reduced order model, the responses from normalized El Centro earthquake would be used. El Centro 1964 earthquake was normalized to 1g. 10% and 80% of the normalized El Centro was used for further analysis. The time history and the acceleration response spectrum of 10% of the normalized El Centro earthquake are plotted in Figure 44, where a_x is the acceleration recorded during the

El Centro earthquake. The spectrum indicates that the structure, with a period of up to approximately 0.6 seconds, has the potential to experience amplification in El Centro earthquakes.

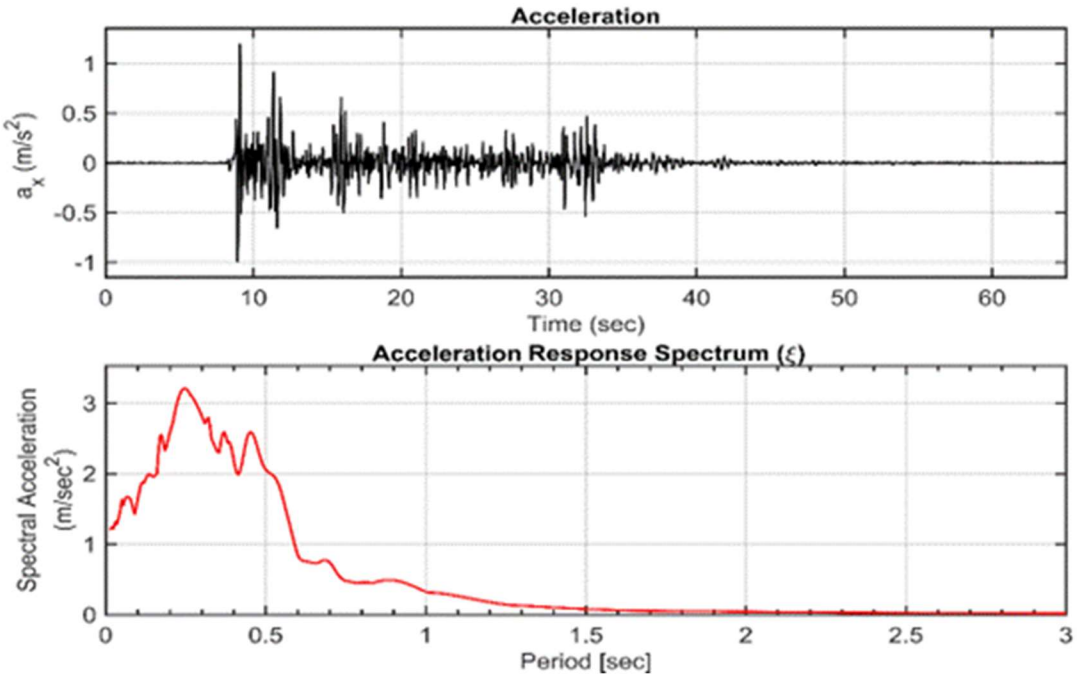

Figure 44: Time history and acceleration response spectrum of normalized 10% El Centro Earthquake

CHAPTER 3 DEVELOPMENT OF THE REDUCED ORDER MODEL

Modeling complex 3D structures in the finite element software to represent the actual structure would require an enormous capacity. This type of simulation model increases the cost and duration of analysis. A reduced order model (ROM) can optimize time and cost, allowing general structural software to create a digital twin and allow non-experts to use the simulations[16]. ROM is a technique used in engineering and applied mathematics to simplify complex mathematical models while retaining their essential dynamic or behavioral characteristics. This is particularly relevant in fields such as control system design, structural analysis, and computational simulations. The idea behind ROM is to reduce the number of degrees of freedom in a system while preserving its key features. This is often done to make simulations or analyses computationally more efficient, as high-dimensional models can be computationally expensive and time-consuming. Reduced order modeling has been used in the field of fluid mechanics[17], circuit simulation[18], and computational aeroelasticity and aerodynamics[19]. Various methods are used to reduce the complex 3D models to a simple model representing the required responses. As the soil box is also a complex structure, creating a representative reduced-order model in a globally accepted software would aid in further study of soil-structure interaction.

3.1 Analysis software – SAP2000

The reduced order model has been developed using Structural Analysis Programming-2000 (SAP2000), developed by Computers and Structures, Inc. (CSI). Even though the software can analyze the structures with foundation boundary conditions as hinge or pin joints, a fixed base design approach is widely accepted. Due to the huge capability, global acceptance, and simplicity of this software, SAP2000 has been selected for developing the

reduced order model. It has predefined soil material that can be used for designing a detailed 3D model of the soil box. However, in a detailed model using the predefined soil properties, the soil needs to be represented as a solid block material with multiple finite solid elements. For the analysis with the soil considered as a 3D soil material mass, a vast and complex finite element model would be required. As an alternative to a detailed 3D model, the soil mass in the box is represented by a reduced order 1D beam model.

3.2 Physical properties of soil

The study of any system under time-dependent loading is achieved by dynamic system analysis. Regarding the dynamics of the soil, properties required to evaluate the nonlinear response of the soil under the imposed ground motion include the shear modulus reduction curves, material damping curves, Poisson's ratio, cyclic shearing stress ratio, and cyclic deformation. For the reduced-order model evaluation, the properties of the soil were studied based on small strain properties using a linear analysis method and for large strain properties using an equivalent-linear model to represent material nonlinear behavior. Linear models based on small strain motions were used to analyze the mode shapes and natural frequencies and to determine initial stiffness. As the soil encounters more significant ground motions, it behaves nonlinearly. This nonlinearity impacts the soil structure interaction due to the softening of the soil and decreased stiffness. The reduced stiffness results in a lessening of the soil's natural frequency. Since soil behaves nonlinearly during most large earthquakes, accurate representation of the nonlinearity of the soil is crucial.

Soil properties for the reduced-order model were characterized based on work carried out at the University of Texas at Austin to study the effect of confinement on the shear modulus

and damping ratio of the soil[20]. Soil samples for that experiment were collected from several drilled geotechnical sites in Northern California, Southern California, South Carolina, and Lotung, Taiwan. Torsional resonant column and cyclic torsional shear tests were carried out to determine the specimen's damping ratio and shear modulus. Statistical analysis was performed using first-order and second-moment Bayesian Method (FSBM). The normalized modulus reduction curves and material damping curves were obtained for several confinement pressures [20]. These curves are used as a basis to extract shear modulus and damping ratio curves for developing the reduced-order model.

3.2.1 Physical properties- Moisture content and void ratio

Several tests were carried out on the soil to determine its dynamic behavior. For this experiment, the soil used was granular sandy soil with an angle of friction of 33°, Poisson's ratio(υ) of 0.3, and a unit weight (γ) of 93 pounds per cubic foot. The earth pressure coefficient of the soil was 0.46. The relative density of the soil was determined to be 43%, and the moisture content was 2.94%. From the plot of shear moduli of sand at different relative densities [21], the value of material coefficient ($K2_{max}$), depending on the void ratio and mean effective stress, was obtained to be 41.49. Based on the compaction of the soil, maximum shear modulus and maximum stiffness have been calculated. Vertical effective stress (σ'_v) is the product of the depth (d) to the unit weight (γ) of the soil. The equations for the mean effective stress (σ'_m), maximum shear modulus (G_{max}), initial young's modulus (E_o) and coefficient of lateral earth pressure at rest (Kb) is mentioned in Table 5. Maximum shear modulus and initial young's modulus are the initial values which would gradually change as per the increase in shear strain and are denoted by G and E respectively.

Table 5: Soil dynamic properties

Thickness of section	Vertical Effective Stress σ'_v		Mean Effective Stress σ'_m	Maximum Shear Modulus G_{max}	Initial Young's Modulus E_o	Coefficient of lateral earth pressure at rest K_b
	d * γ		$\frac{\sigma'_v(1+2K_o)}{3}$	$1000\ K2_{max}\ (\sigma'_m)^{0.5}$	G_{max}* [2(1+ υ)]	[2G(1+υ)/ {3(1-2υ)}]
ft	psf	atm	psf	psf	psf	psf
0.9583	44.56	0.021	28.38	221037.69	574697.98	478914.99
0.7708	124.97	0.059	79.59	370153.84	962400.00	802000.00
0.7708	196.66	0.093	125.25	464339.28	1207282.14	1006068.45
0.7708	268.34	0.127	170.91	542409.51	1410264.72	1175220.60
0.7708	340.03	0.161	216.57	610577.74	1587502.13	1322918.44
0.7708	411.72	0.195	262.23	671864.78	1746848.42	1455707.02
0.7708	483.41	**0.228**	307.88	728010.57	1892827.47	1577356.22
0.7708	555.09	0.262	353.54	780125.94	2028327.45	1690272.88
0.7708	626.78	0.296	399.20	828971.40	2155325.65	1796104.71
0.7708	698.47	0.330	444.86	875094.68	2275246.16	1896038.46
0.7708	770.16	0.364	490.52	918905.76	2389154.97	1990962.48
0.7708	841.84	0.398	536.18	960721.03	2497874.68	2081562.23
0.7708	913.53	**0.432**	581.83	1000790.69	2602055.79	2168379.82

3.2.2 Shear modulus reduction curve

Shear modulus is the measure of elastic shear stiffness of the material. The shear modulus reduction curves with respect to the shear strain of the soil are dependent on the soil confinement due to the soil overburden pressure. The overburden pressure, σ'_v, as calculated in Table 5, for the top 7 layers of the soil was calculated to be less than 0.25 atm, and the maximum overburden pressure at the lowest layer of the soil box was 0.43 atm. As

per the study of the development of normalized modulus reduction and material damping curves carried out by M. B. Darendeli, the curves for the confinement pressure of 0.25 atm, 1 atm, 4 atm and 16 atm were available[20]. As the soil box had the maximum pressure of 0.432 atm pressure, 0.25 atm and 1 atm curves were abstracted from the research for further study and development of the ROM. The shear modulus reduction curve, damping ratio curve and shear stress-strain plot for the top seven layers of the soil was obtained from the plot of 0.25 atm and for the lower six layers, curves were interpolated from 0.25 atm to 1 atm to obtain the plot of 0.43 atm. The shear modulus of the soil layers is maximum at its initial unstrained condition, which was determined with respect to the depth of the soil. When the model is subjected to the ground motions, soil layers experience different strains. As the soil experiences ground motion and starts to soften, its shear properties start to change. The shear modulus reduction curve indicates the variation of soil shear modulus with the shear strain of the soil. These changes in the shear strain could correspond to the shear modulus reduction, as demonstrated in Figure 45.

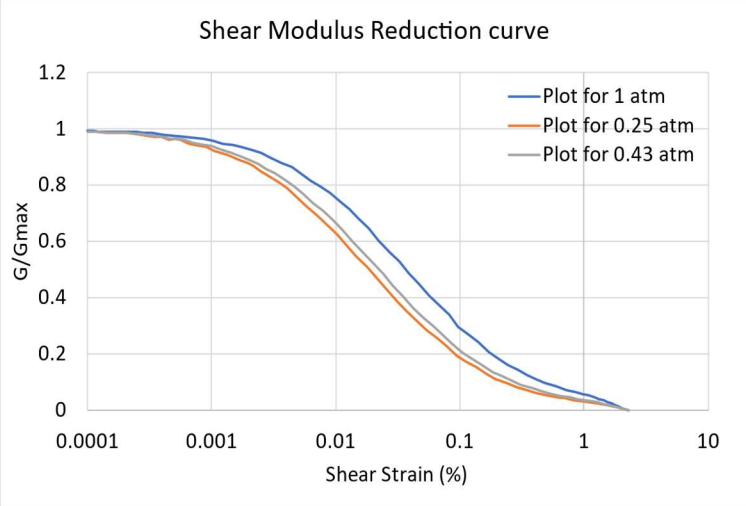

Figure 45: Darendeli's shear modulus reduction curve with effect of confinement

3.2.3 Damping ratio curve

The curve for the damping ratio was obtained following the same steps of shear modulus reduction curve. The plot of the damping ratio includes two curves obtained for 0.25 atm and 0.43 atm confinement pressure as observed in Figure 46. The curve has been used to develop and refine the ROM.

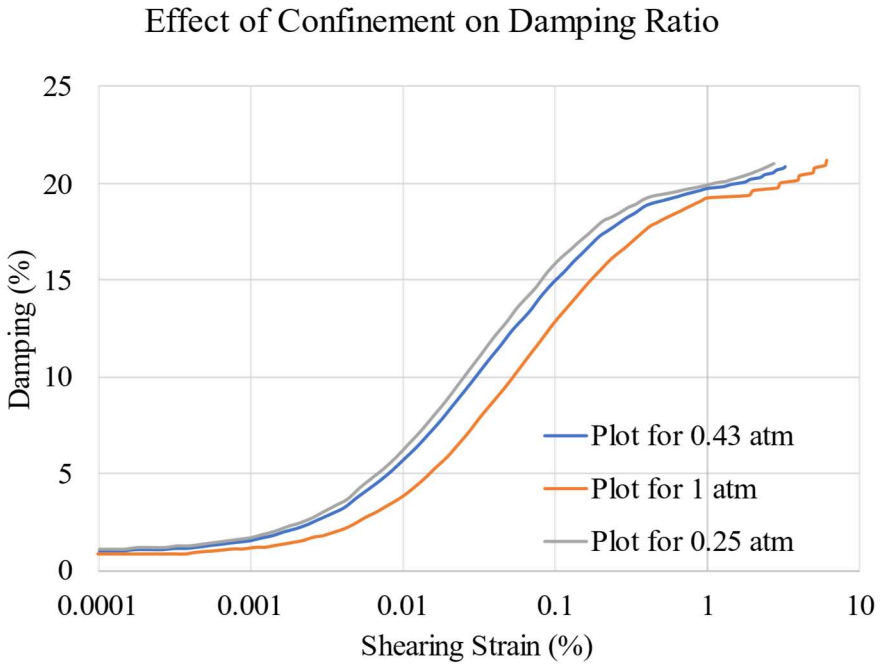

Figure 46: Darendeli's damping ratio curve with effect of confinement

3.2.4 Stress-strain curve

As shear modulus is the ratio of shear stress to shear strain, the shear stress has been calculated as a product of shear modulus and shear strain [20]. From the chart of shear modulus reduction curve, assuming maximum shear modulus as unity, the data for the shear modulus and the shear strain were obtained. These values were multiplied to obtain the corresponding shear stress of the soil. The data of the shear modulus reduction curve has

been used to obtain the shear stress to shear strain curves for two overburden pressure ranges observed in Figure 47. The blue solid line represents the shear stress-strain curve for the lower six soil layers with the overburden pressure of 0.43 atm (913 psf). The orange dotted line would be defined for the shear stress-strain curve for the upper seven soil layers with the confinement pressure of 0.25 atm (530 psf). The stress-strain plot obtained is used as the input parameter for developing the reduced-order model. As the shear strain of the soil increases, the stiffness decreases resulting in higher yielding of the soil.

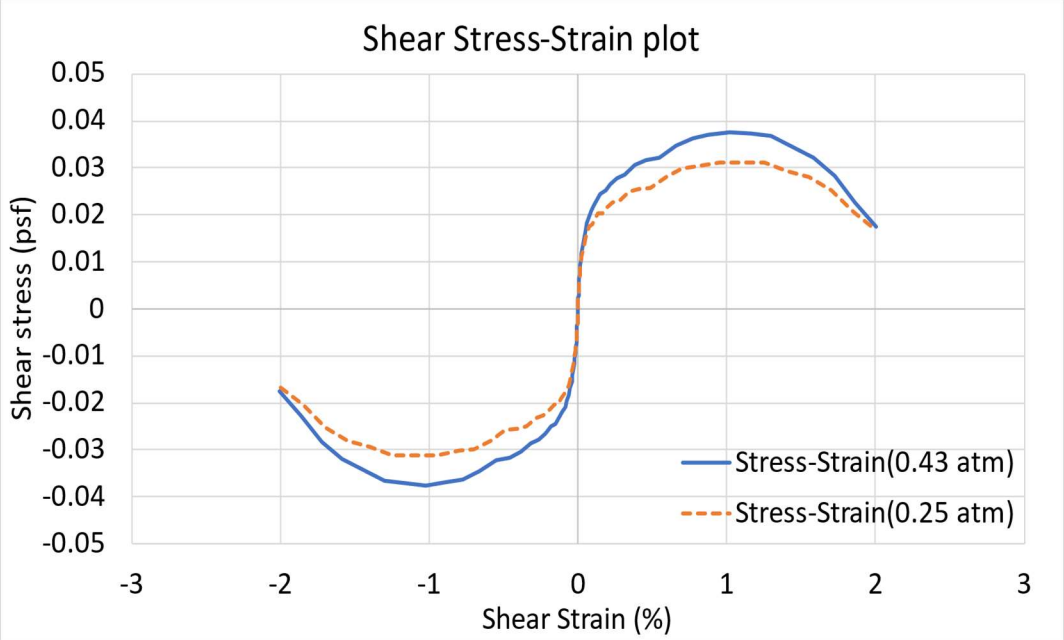

Figure 47: Shear stress-strain curve for different confinement pressures

3.3 Basis for utilization of a shear beam model

The maximum and minimum pressure envelopes obtained from the data of pressure cells placed in the soil box plotted in Figure 48 to Figure 50 emphasize that the response of the soil box when it is shaken with up to the normalized 50% El Centro ground motion with 0.33g, can be expected to have linear response. Beyond this, the soil would behave nonlinearly. Similar results can be observed from the pressure cells in all three directions.

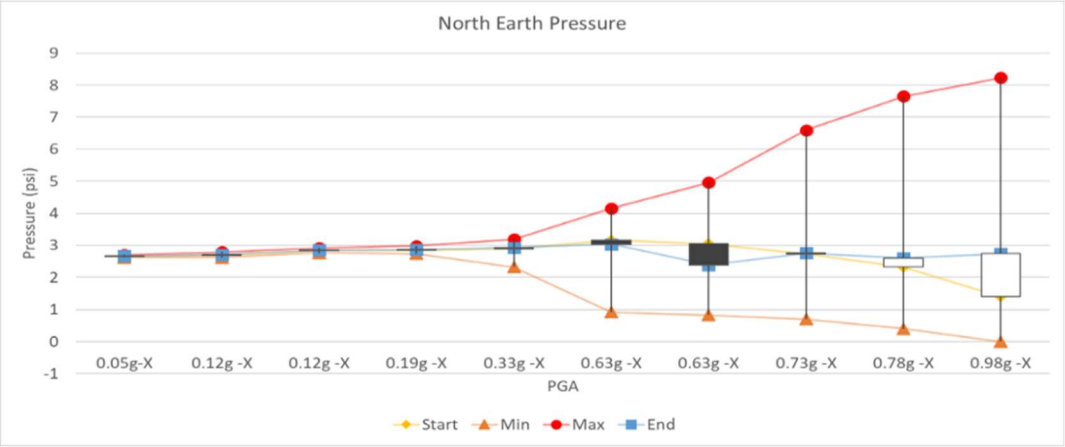

Figure 48: Earth pressure cell result towards North

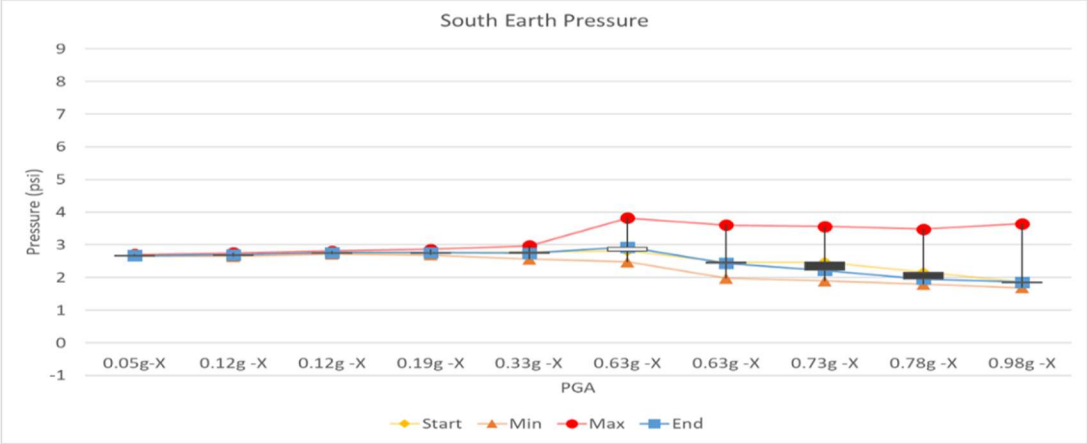

Figure 49: Earth pressure cell result towards South

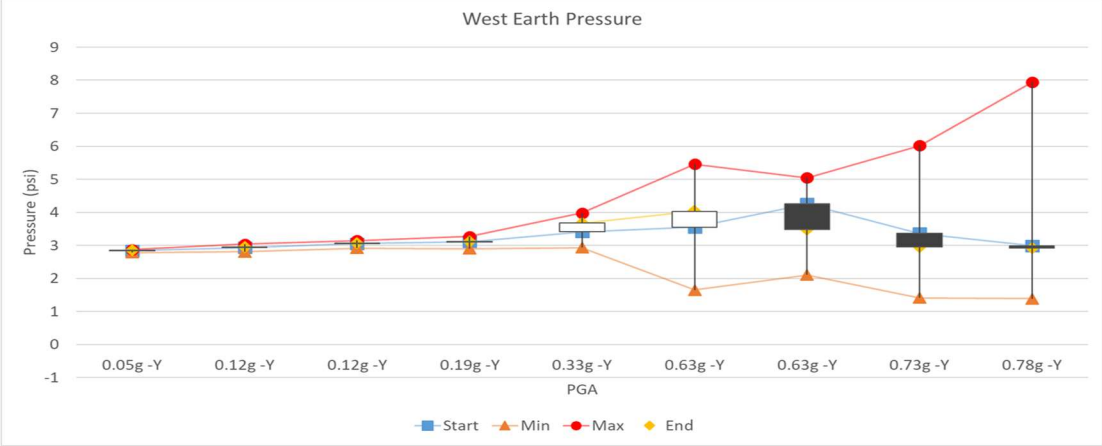

Figure 50: Earth pressure cell result towards West

3.4 Development of the equivalent Timoshenko beam properties

From the analysis of the data extracted from the experiment of the soil box with soil, it was found that the motion of the soil box was dominated by the soil. Due to the minimal impact of the soil box on the movement of the compacted soil, the soil box was not considered while developing the reduced-order model. As the soil in the soil box is shear dominant and the mode shape of the soil box with soil was equivalent to a shear beam, the primary representation for the development of a reduced order model is considering the column as a Timoshenko beam. The lateral deflection *v* on the beam subjected to the shearing forces and associated moments is given by Timoshenko shear beam theory as:

$$v = v_b + v_s \qquad [22]$$

where,

v_b = lateral deflection due to bending strain

v_s = additional deflection due to the shear strain

$$\frac{dv_s}{dx} = \frac{-S}{GA_s} \qquad [22]$$

For developing a shear beam, one end of the soil column has been considered fixed, and the other end restrained vertically. A 15-inch-long column was created, and pushover analysis was carried out for this section. The deformation of this model, as observed in Figure 51, confirms that the model deforms as a shear beam[15]. With the same principle, a soil column with the intermediate nodes at 9 inches each and the top of layer of 12 inches was developed with the total height of 120 inches. The intermediate nodes were restrained vertically, and the base was fixed. The octagonal box was modeled as having a circular

cross-section to simplify the model. The cross-section area of the soil box for the experiment was 463 ft^2, so a section with the same cross-section area was created. A column with 13 layers was considered as the final model for the analysis. A pushover analysis was repeated for the whole height of the soil column to verify the model acts as a shear beam. The mode shapes of the experimental model of the soil box with soil and the deformation of the modeled soil column were found to be comparable, as observed in Figure 52. As this model represented the Timoshenko beam [15], the generated column model could represent the soil box system with compacted soil.

Figure 51: Deformation of the soil column at adjacent nodes

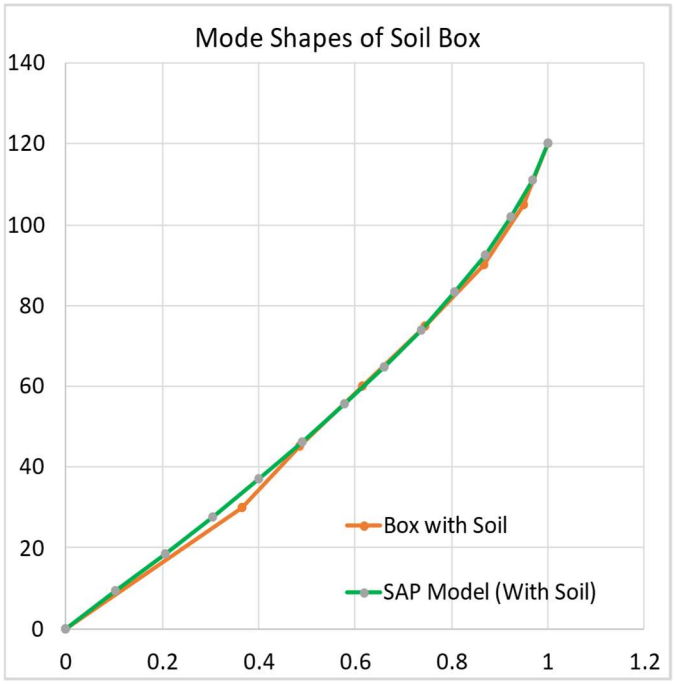

Figure 52: Mode Shape comparison of Soil Box with Soil and Shear Beam

The subsequent step for the analysis is characterizing the column to represent the soil confined inside the box during the experiment. The physical properties of the soil calculated in section 3.2.1 would be the input parameters to represent the soil at its initial condition as seen in the appendices. For the first simulation, the maximum shear modulus

as mentioned in Table 5 for each layers and minimum damping ratio of 1.2% were considered. Assuming an equivalent linear method of analysis, the reduced-order model was simulated with the normalized 10% and 80% El Centro ground motions. The natural frequency, mode shape, displacement, and acceleration of the ROM at the top of the box are recorded for further analysis.

3.5 Equivalent linear iterative model updates for nonlinear response

As the El Centro earthquake motions were introduced in the reduced order model, the soil strain levels increased. The model undergoes various strain intensity during any ground motions. The maximum value of strain attained during the earthquake motion is observed for a few cycles. To avoid overstraining of the model and represent the average strain for the subsequent iterations, 65% of the maximum observed strain was estimated to be the effective strain [23]. For effective strains attained at each level, the modulus of elasticity and damping ratio were recalculated, and the simulation was repeated with the revised values. The repetition was terminated when the change in strain was found to be negligible with additional iterations.

When the soil box was excited with a 10% normalized El Centro earthquake (0.12g), after a slight reduction in the shear modulus during the first iteration, negligible change in strain was observed. As the excitation level was increased to 80% normalized El Centro motion, the model encountered nonlinearity, with the effective shear strain exceeding 2%. The reduction of shear modulus for the yielded soil reached 0.07% of the maximum shear modulus when the model strained by 2.3%. Figure 53 indicates the maximum strain attained at the final condition for both linear and nonlinear loading conditions. The plot is obtained from the research by Darendeli is summarized with the curves for 0.25 atm and

0.43 atm confinement pressure for the development of the reduced order model. For this linear model, at the strain of 0.0043%, the shear modulus was reduced to 80% of the initial small strain modulus.

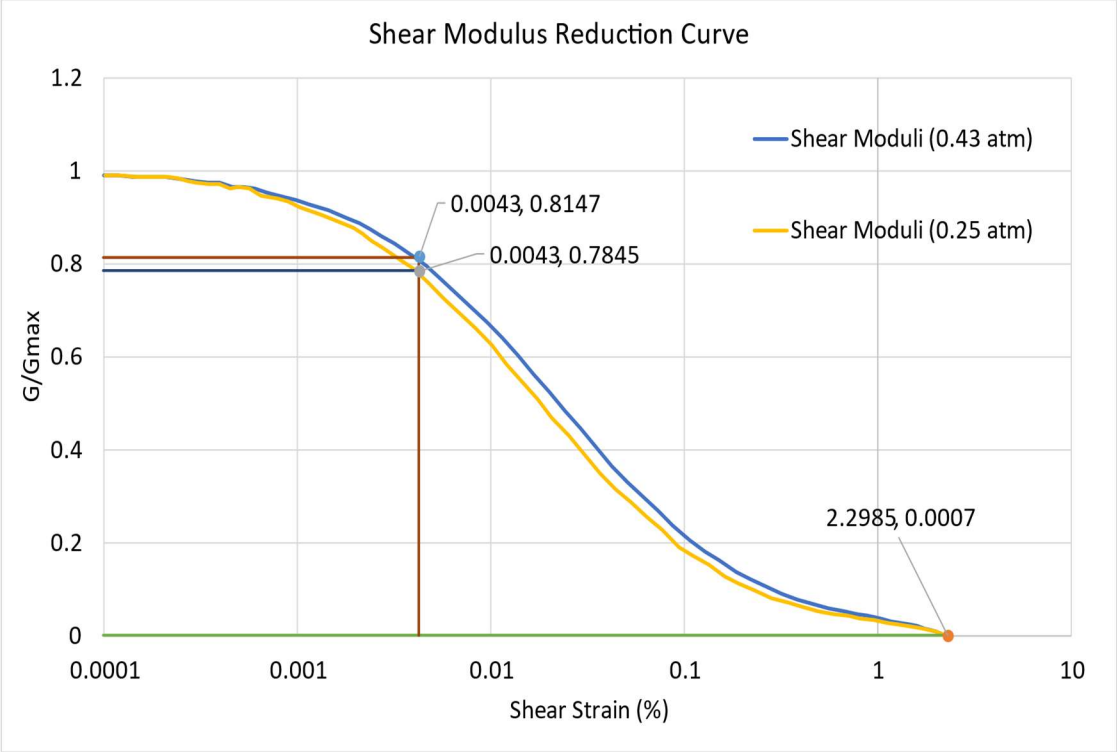

Figure 53: Shear modulus reduction curve for the maximum strain level achieved in linear and nonlinear motions

The damping ratio curves in relation to the confinement pressures obtained from the study carried out by Darendeli has been summarized for 0.25 atm and 0.43 atm pressure curves with respect to the data of soil box used for the development of the reduced order model. The initial value of the damping ratio of the model before shaking with ground motions was set to the minimum value of 1.2% for all overburden pressures as obtained from Figure 54. The model was analyzed, and the damping ratio for each layer was iterated based on the effective strain model attained. Figure 55 compares the final shear strains on each layer

obtained from experimental results of El Centro 10% causing linear response and from the reduced order model simulated with the same earthquake motion. At the final effective strain of 0.0043% for the linear model, the damping ratio was increased from 1.2% to 4.5%, as indicated in Figure 54. Similarly, for the effective strain of 2.3%, the damping ratio in the nonlinear model, excited with 80% El Centro ground motion, reached up to 20.74%.

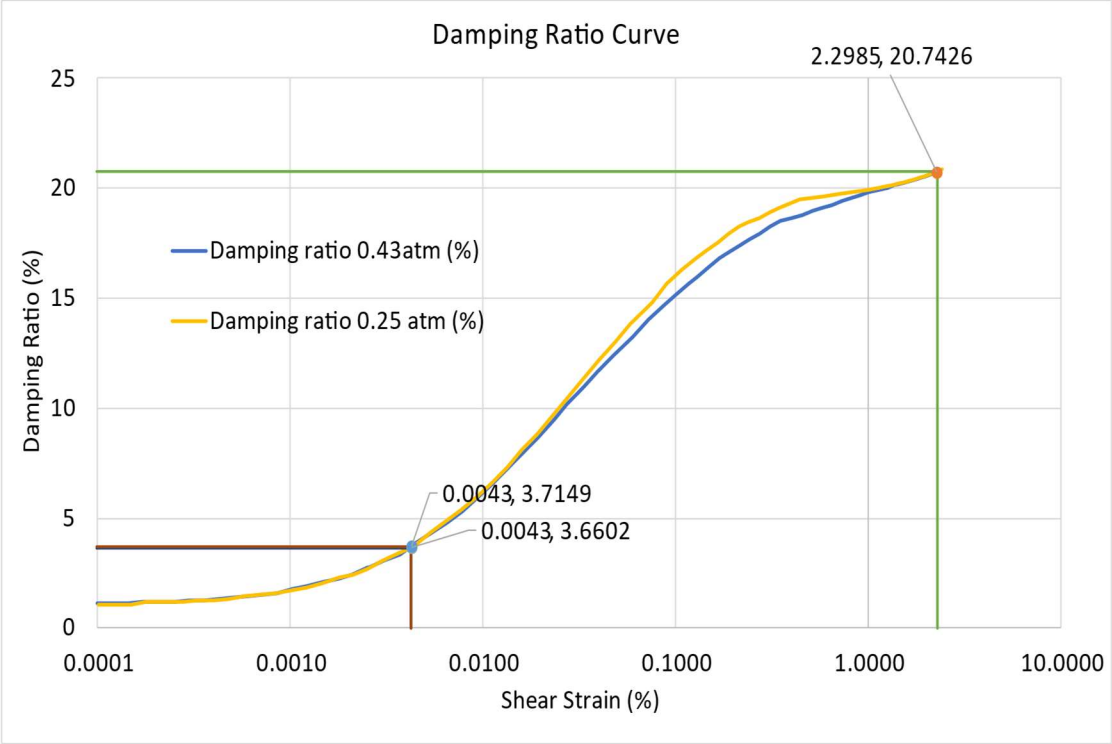

Figure 54: Damping ratio curve for the maximum strain level attained in linear and nonlinear motions

The effective strain at each level obtained from the reduced order model and the strain of soil during the linear and nonlinear ground motion experiment are plotted in Figure 55 and Figure 56. The effective strain pattern observed from the simulation is similar to the experimental strain for both linear and nonlinear responses. However, some discrepancies could have been observed due to the location at which readings were taken. For the experimental model, the data from the Novotechnik placed at the face of the soil box was

used to obtain the strain. Novotechnik linear position sensors provide high quality data compared to string potentiometers. Strain from the reduced order model would represent the strain at the center of the soil box.

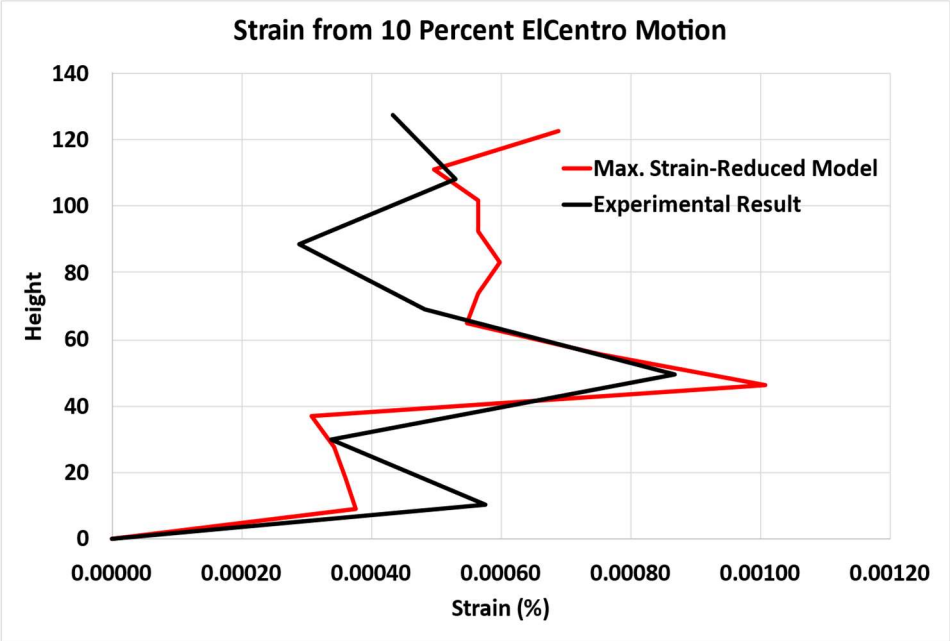

Figure 55: Strain comparison for linear analysis

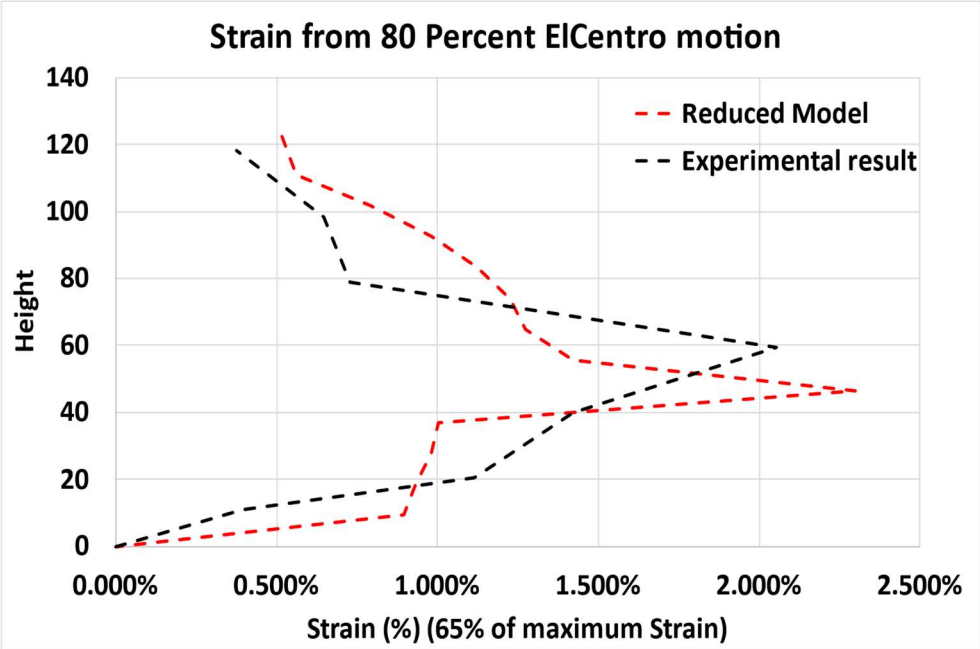

Figure 56: Strain comparison with experimental strain on each soil level

Table 6 represents the initially defined maximum modulus of elasticity along with the final reduced modulus of elasticity and respective shear modulus based on the effective strain achieved at each layer. These final moduli of elasticity were achieved after subsequent iterations and signify the development of the reduced-order model.

Table 6: Shear modulus reduction based on strain

Actual Depth (ft)	Initial values for ROM		Linear SAP ROM		Nonlinear SAP ROM	
	Shear Modulus	Modulus of Elasticity	Shear Modulus	Modulus of Elasticity	Shear Modulus	Modulus of Elasticity
0.96	221037.69	574697.98	13097.19	34052.71	54748.11	142345.08
1.73	370153.84	962400.00	62930.39	163619.01	83951.38	218273.58
2.50	464339.28	1207282.14	77138.53	200560.19	73015.73	189840.89
3.27	542409.51	1410264.72	84492.47	219680.43	65444.81	170156.51
4.04	610577.74	1587502.13	85421.41	222095.68	60792.68	158060.97
4.81	671864.78	1746848.42	109064.6	283568.07	58088.17	151029.25
5.58	728010.57	1892827.47	134389.6	349412.96	58175.13	151255.35
6.35	780125.94	2028327.45	81672.02	212347.25	53706.73	139637.49
7.13	828971.40	2155325.65	85501.54	222304.01	33531.6	87182.17
7.90	875094.68	2275246.16	267863.9	696446.25	115932.2	301423.62
8.67	918905.76	2389154.97	287973.4	748730.89	123826.3	321948.47
9.44	960721.03	2497874.68	295768.9	768999.05	137044.2	356314.80
10.21	1000790.69	2602055.79	299333.6	778267.41	150424.9	391104.73

CHAPTER 4 RESULT AND DISCUSSION

This chapter presents the results obtained from the shake table test of the fully loaded soil box and along with a comparison with the reduced-order model.

4.1 Model validation for natural mode shapes

The mode shapes of the empty soil box, soil box with compacted soil, and developed reduced order model were compared. The natural mode shape of the experimental model was found to be comparable to the shear beam from the reduced order model and was different from the mode shape of the empty soil box, as observed in Figure 57.

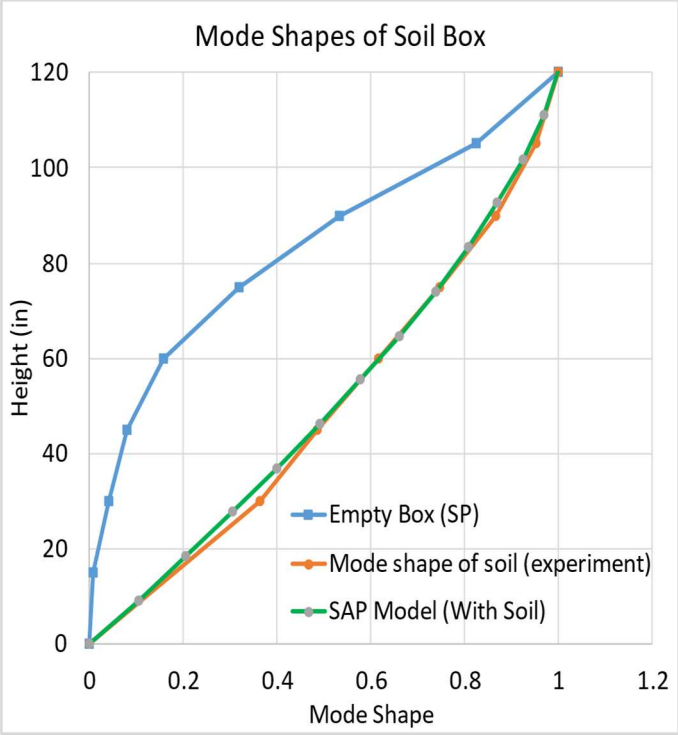

Figure 57: Mode shape of soil box compared to reduced order model

A similar pattern of response was evidenced in Figure 58 when the frequency contents from the experimental data were compared. Most of the soil box natural frequencies were observed as the input motion encompassed frequency content (up to 20 Hz) spanning all

these natural frequencies. The fundamental frequency of the empty box was approximately 2 Hz. After compacting the soil box with soil, a fundamental frequency of 11.9 Hz was observed. After yielding, the frequency of the soil-filled box dropped to 8 Hz, a reduction of almost 4 Hz.

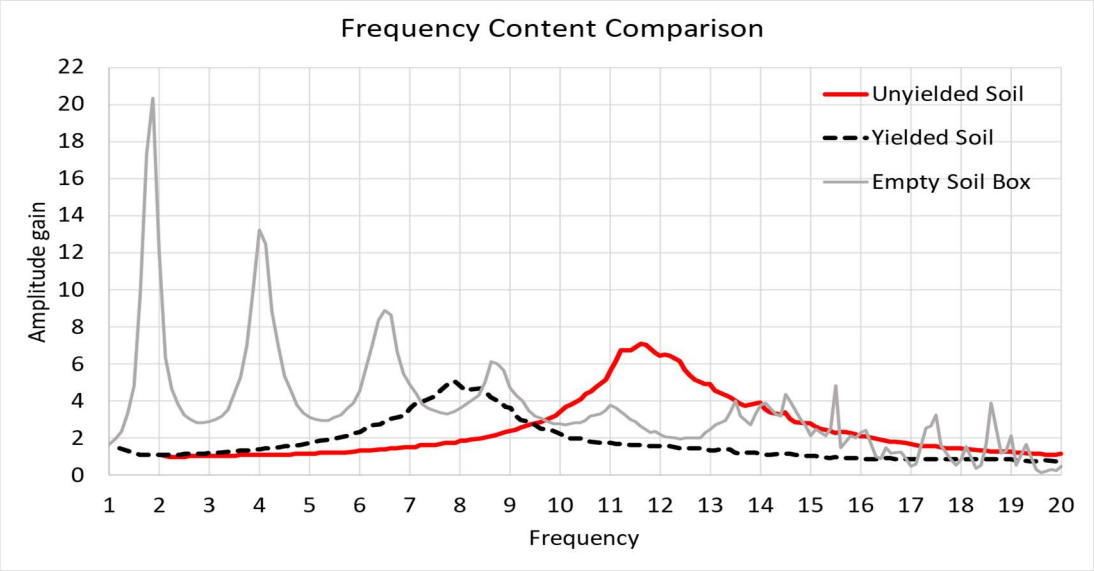

Figure 58: Frequency content comparison of soil box with and without soil

The modal period, along with the frequency content of the reduced order model, is tabulated in Table 7. The fundamental frequency of 11.9 Hz in the experiment is comparable to 10.9 Hz from the SAP model. The second natural frequency was not observed experimentally. However, from the reduced order model, the second it was observed to be 23.06 Hz.

It can also be perceived that the fundamental frequency of the reduced order model decreased from 10.887 Hz to 4.16 Hz when the soil experienced nonlinearity. The reduction in frequency due to soil yielding was captured by the reduced order model. However, it was not able to capture the magnitude of the reduced frequency. A notable difference,

though, between the initial and final frequency of the soil box obtained from the experiment and the simulation model indicates that the model has been significantly softened.

Table 7: Model period and frequency comparison for reduced order model

Modal periods and frequencies				**Frequency**	
Output Case	**Step Type**	**Step Num**	**Period**	**Initial**	**Final**
Text	Text	Unitless	Sec	Hz	Hz
MODAL	Mode	1	0.0919	10.8869	4.1596
MODAL	Mode	2	0.0434	23.0628	12.2719
MODAL	Mode	3	0.0271	36.8592	19.2434
MODAL	Mode	4	0.0204	49.0725	25.7231
MODAL	Mode	5	0.0167	60.0495	32.2330
MODAL	Mode	6	0.0139	71.7954	38.2322
MODAL	Mode	7	0.0119	83.9119	43.8620
MODAL	Mode	8	0.0105	95.4953	48.2405
MODAL	Mode	9	0.0094	106.3779	53.0228
MODAL	Mode	10	0.0086	116.8448	58.1041
MODAL	Mode	11	0.0079	127.2627	61.4883
MODAL	Mode	12	0.0072	138.0237	65.4757

4.2 Model validation for simulated earthquake motions

The time history recorded from the accelerometer at the top of the soil column from the experiment are compared to the acceleration obtained at the top of the reduced order model in Figure 59 and Figure 60. Figure 59 indicates the time history of the experimental and

reduced order model for 10 percent normalized El Centro ground motion with linear response. These time histories are observed to have comparable peak ground accelerations and comparable acceleration patterns without any phase shifts.

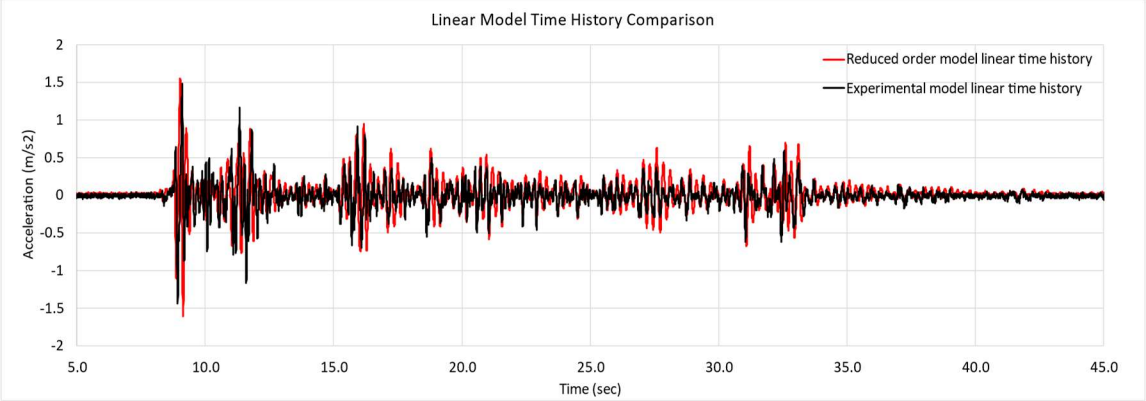

Figure 59: Linear response time histories

The nonlinear response time history obtained from the acceleration peaks at the top of the soil as a result of 80 percent normalized El Centro ground motion is represented by Figure 60. The reduced order model resulted in higher peak ground accelerations than those observed in the experimental data. This suggests that the model has calculated a higher degree of soil softening compared to the actual experimental conditions.

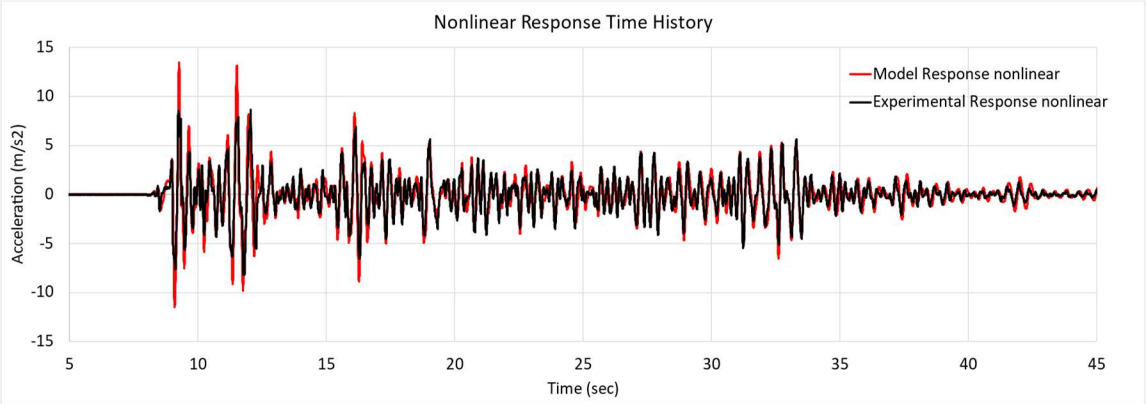

Figure 60: Nonlinear response time histories

From Figure 48-50, it can be observed that the bulk motion of the soil impacting the pressure cells attached to the surface of the box is low for the linear motions below 50

percent El Centro and is high for the higher amplitude ground motions. This interaction of the soil to the box in the experiment is not considered for the reduced order model. As the low amplitude motions have a smaller impact, the time history seems comparable. As the soil reaches non-linearity, the soil pounds to the box surface during the experiment, reducing its acceleration. However, this phenomenon is not considered for the reduced order model, resulting in the observation of a higher acceleration peak of the reduced order model.

4.3 Acceleration response spectrum comparison

From the acceleration response spectrum obtained from the reduced order model, it can be observed that the model takes multiple iterations to be comparable to the acceleration response spectrum obtained from the experiment. The acceleration response spectrum for the experimental outputs compared to the model response spectrum is illustrated in Figure 61The comparison of the acceleration response spectrum for the linear and nonlinear ground motions would be difficult because of the low and high-intensity ground motions; the responses are normalized to the 10 percent El Centro earthquake representing the lower-intensity ground motion.

The solid lines in Figure 61 indicate the linear response spectrum, and the dotted lines indicate the nonlinear response spectrum. The black line indicates the experimental responses, and the red lines indicate responses from the developed reduced-order simulation model. The period of the unyielded soil box system is observed to be approximately 0.25 seconds. As the soil yielded, the period of the system elongated to 0.38 seconds. The peaks of nonlinear responses are observed with periods longer than the linear responses, indicating that the model softens after going through the more significant ground

motion. The peaks observed in the acceleration response spectrum of the reduced order model emulate the spectrum of the experimental model. Also, the peak ground acceleration of the experimental soil box before yielding is equal to that of the reduced-order model. The peak ground acceleration of the simulated soil column model after yielding is higher than that of the experimental response. As the ROM does not represent a more visible degree of small stiffness and damping contributions from the soil box and soil interactions, the amplitude of the spectrum from the ROM has been higher than the spectral amplitude obtained from the experiment.

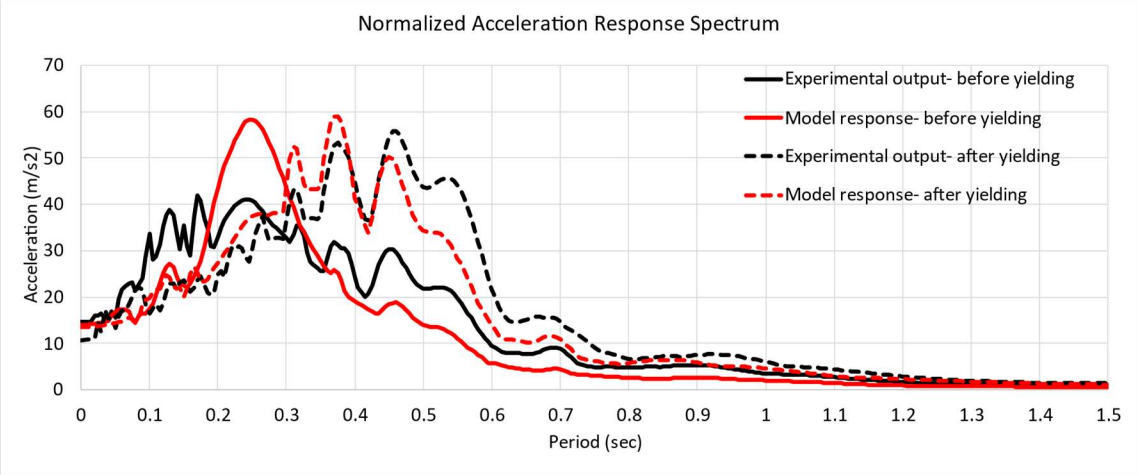

Figure 61: Normalized acceleration response spectrum.

CHAPTER 5 CONCLUSION

The analysis of the experimental response obtained from the empty soil box concluded that the empty soil box tends to have Euler behavior [15]. After filling the soil box with compacted soil, the system behaved as a shear beam response as designed [15]. The reduced order model was developed to resemble the response of the soil box filled with compacted soil, excluding the soil box envelope. It was concluded that a Timoshenko beam can be used to develop the reduced-order model of the soil column by assuming the compacted soil as a cantilever beam.

The comparison of the response properties of the experimental soil box model with compacted soil and its reduced order model is conclusively listed as follows:

1. The mode shape of the simulated reduced order model was found to have a higher resemblance to that of the experiment. So, this reduced-order model can be applicable to predict the expected mode shapes of the soil column.
2. The reduced order model captured the softening of the soil. The frequency content of the soil box after yielding had a significant reduction from that before yielding when compared for both experimental and simulation models.
3. The acceleration response spectrum of the reduced order model was observed to resemble the spectrum obtained from the experiment. The reduced-order model can provide a valid comparison of the acceleration response spectrums.
4. The time histories of the soil box before yielding had a remarkable resemblance to the soil column developed. After yielding, the soil column from ROM showed higher peak ground acceleration, indicating somewhat higher softening.

5. The difference in the natural frequencies between the experimental and reduced order model of the soil box after yielding signifies that the developed reduced order model cannot capture the exact frequency content of the soil box after it yields.
6. The reduced order model developed can be a basis for estimating the acceleration response of the ground motions and predicting the nature of the acceleration response to ground motions, helping further study of soil structure interaction.

REFERENCES

[1] "What causes earthquakes? - British Geological Survey." Accessed: Apr. 19, 2023. [Online]. Available: https://www.bgs.ac.uk/discovering-geology/earth-hazards/earthquakes/what-causes-earthquakes/

[2] S. L. Kramer, "Geotechnical Earthquake Engineering."

[3] N. S.K, "Soil-Structure Interaction- Effects, Analysis and Applications in Design," The Constructor - Building ideas. Accessed: Jan. 14, 2024. [Online]. Available: https://theconstructor.org/structural-engg/soil-structure-interaction-effects-analysis-applications/17778

[4] M. E. Rodriguez, "The interpretation of cumulative damage from the building response observed in Mexico City during the 19 September 2017 earthquake," *Earthquake Spectra*, vol. 36, no. 2_suppl, 2020, doi: 10.1177/8755293020971307.

[5] M. Lou, H. Wang, X. Chen, and Y. Zhai, "Structure-soil-structure interaction: Literature review," *Soil Dynamics and Earthquake Engineering*, vol. 31, no. 12, pp. 1724–1731, Dec. 2011, doi: 10.1016/j.soildyn.2011.07.008.

[6] G. Housner, "Calculation of the Earthquake Response Spectrum," 1941. Accessed: Jul. 22, 2023. [Online]. Available: https://www.curee.org/wp-content/uploads/2022/01/1998-CUREE_excerpt.pdf

[7] P. Kamatchi, G. V. Ramana, A. K. Nagpal, and N. R. Iyer, "Modelling Propagation of Stress Waves through Soil Medium for Ground Response Analysis," *Engineering*, vol. 05, no. 07, pp. 611–621, 2013, doi: 10.4236/eng.2013.57073.

[8] A. H. Hadjian, W. S. Tseng, N. C. Tsai, and C. Y. Chang, “International Conferences on Recent Advances in Geotechnical Earthquake Engineering and Soil Dynamics,” 1991. [Online]. Available: https://scholarsmine.mst.edu/icrageesd/02icrageesd/session05/46

[9] H. F. Xiang, A. R. Chen, and Z. X. Lin, “An introduction to the Chinese wind-resistant design guideline for highway bridges,” *Journal of Wind Engineering and Industrial Aerodynamics*, vol. 74–76, pp. 903–911, Apr. 1998.

[10] X. Lu, P. Li, B. Chen, and Y. Chen, “Numerical Analysis of Dynamic Soil-Box Foundation-Structure Interaction System,” *Journal of Asian Architecture and Building Engineering*, vol. 1, no. 2, pp. 9–16, 2002.

[11] A. Bistani *et al.*, “Design of a Large-Scale Biaxial Soil-Box for Seismic Soil-Structure-Interaction Studies,” Los Angeles, California, Jun. 2018. [Online]. Available: https://www.researchgate.net/publication/326160904

[12] I. Buckle, D. Istrati, P. Laplace, R. Motamed, and R. Siddharthan, “Design, Fabrication and Commissioning of a Large Laminar Soil Box and Shake Table,” 2023.

[13] I. Buckle, S. Elfass, and P. Laplace, “ A Modern Computational Framework for the Nonlinear Seismic Analysis of Nuclear Facilities and Systems: Design, Fabrication and Commissioning of a Large Laminar Soil Box and Shake Table ,” Civil Engineering Department, Report No. CCEER-23-02, University of Nevada, Reno, August 2023.

[14] K. Bin Ngadimon, “Design and Simulation of Hydraulic Shaking Table,” 2006.

[15] M. Perrault, P. Gueguen, A. Aldea, and S. Demetriu, "Using experimental data to reduce the single-building sigma of fragility curves: Case study of the BRD tower in Bucharest, Romania," *Earthquake Engineering and Engineering Vibration*, vol. 12, no. 4, pp. 643–658, Dec. 2013, doi: 10.1007/s11803-013-0203-z.

[16] "What is a Reduced Order Model and Its Role in Product Development_".

[17] Y. Lang, A. Malacina, L. Biegler, S. Munteanu, J. Madsen, and S. Zitney, "Reduced Order Model Based on Principal Component Analysis for Process Simulation and Optimization†," *Energy & Fuels*, vol. 23, Mar. 2009, doi: 10.1021/ef800984v.

[18] Z. Bai, P. M. Dewilde, and R. W. Freund, "Reduced-Order Modeling," *Handbook of Numerical Analysis*, vol. 13, pp. 825–895, Jan. 2005, doi: 10.1016/S1570-8659(04)13009-3.

[19] D. J. Lucia, P. S. Beran, and W. A. Silva, "Reduced-order modeling: new approaches for computational physics," *Progress in Aerospace Sciences*, vol. 40, no. 1–2, pp. 51–117, Feb. 2004, doi: 10.1016/J.PAEROSCI.2003.12.001.

[20] M. B. Darendeli, "Development of a New Family of Normalized Modulus Reduction and Material Damping Curves."

[21] "Soil Moduli and Damping Factors for Dynamic Response Analyses," 2010.

[22] J. S. Przemieniecki and N. York, "Theory of Matrix Structural Analysis."

[23] S. J. Lasley, R. A. Green, and A. Rodriguez-Marek, "Comparison of equivalent-linear site response analysis software," in *NCEE 2014 - 10th U.S. National*

Conference on Earthquake Engineering: Frontiers of Earthquake Engineering, Earthquake Engineering Research Institute, 2014. doi: 10.4231/D3P26Q42R.

APPENDICES

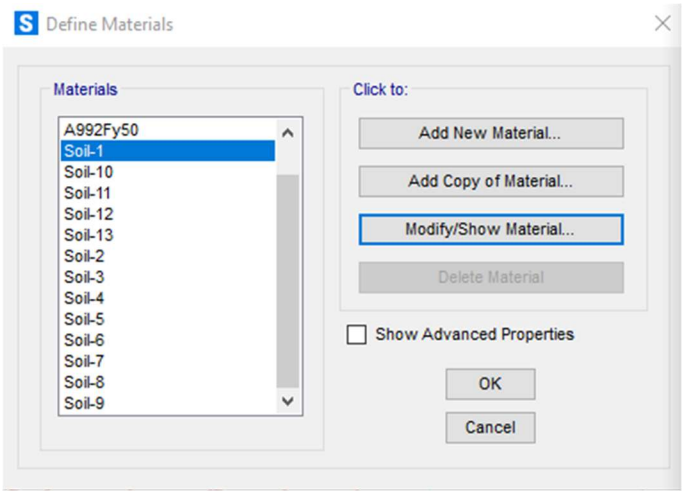
Define Materials
Materials
A992Fy50
Soil-1
Soil-10
Soil-11
Soil-12
Soil-13
Soil-2
Soil-3
Soil-4
Soil-5
Soil-6
Soil-7
Soil-8
Soil-9
Click to:
Add New Material...
Add Copy of Material...
Modify/Show Material...
Delete Material
Show Advanced Properties
OK
Cancel


Material Property Data
X
Material Name
Soil-1
Material Type
Other
Symmetry Type
Isotropic
Modulus of Elasticity
E
574698.
Weight and Mass
Weight per Unit Volume
93.
Mass per Unit Volume
2.8905
Units
lb, ft, F
Advanced Material Property Data
Uniaxial Nonlinear Data...
Material Damping Properties...
Coupled Nonlinear Data...
Time Dependent Properties...
Poisson
U
0.3
Coeff of Thermal Expansion
A
6.500E-06
Shear Modulus
G
221037.68
OK
Cancel

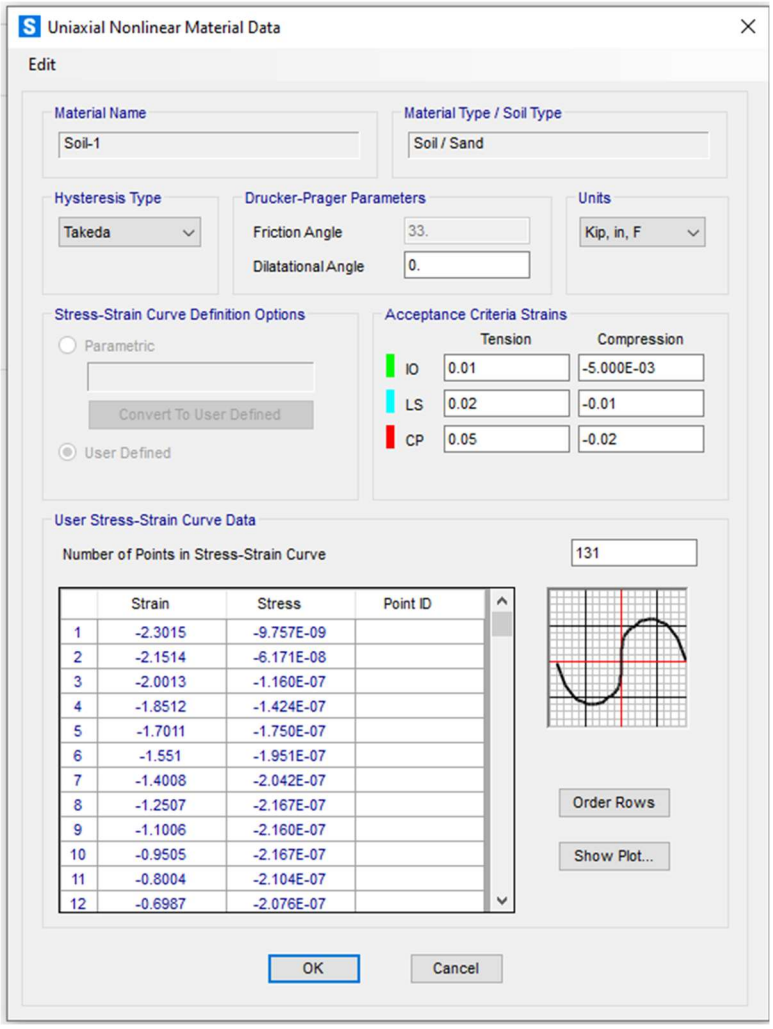
Uniaxial Nonlinear Material Data
Edit
Material Name
Soil-1
Material Type / Soil Type
Soil / Sand
Hysteresis Type
Takeda
Drucker-Prager Parameters
Friction Angle
33.
Dilatational Angle
0.
Units
Kip, in, F
Stress-Strain Curve Definition Options
Parametric
Convert To User Defined
User Defined
Acceptance Criteria Strains
Tension
Compression
IO
0.01
-5.000E-03
LS
0.02
-0.01
CP
0.05
-0.02
User Stress-Strain Curve Data
Number of Points in Stress-Strain Curve
131
Strain
Stress
Point ID
1 -2.3015 -9.757E-09
2 -2.1514 -6.171E-08
3 -2.0013 -1.160E-07
4 -1.8512 -1.424E-07
5 -1.7011 -1.750E-07
6 -1.551 -1.951E-07
7 -1.4008 -2.042E-07
8 -1.2507 -2.167E-07
9 -1.1006 -2.160E-07
10 -0.9505 -2.167E-07
11 -0.8004 -2.104E-07
12 -0.6987 -2.076E-07
Order Rows
Show Plot...
OK
Cancel

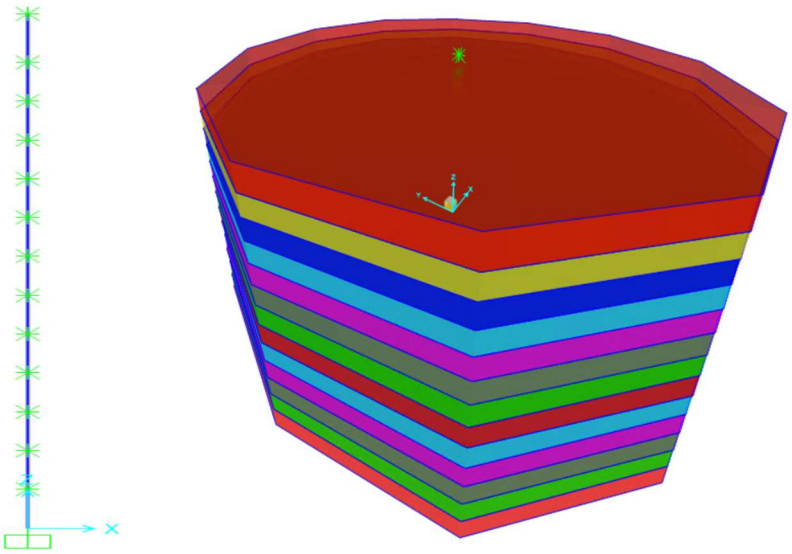


Motor #1:
Slow circles, no box deformation


25-5T

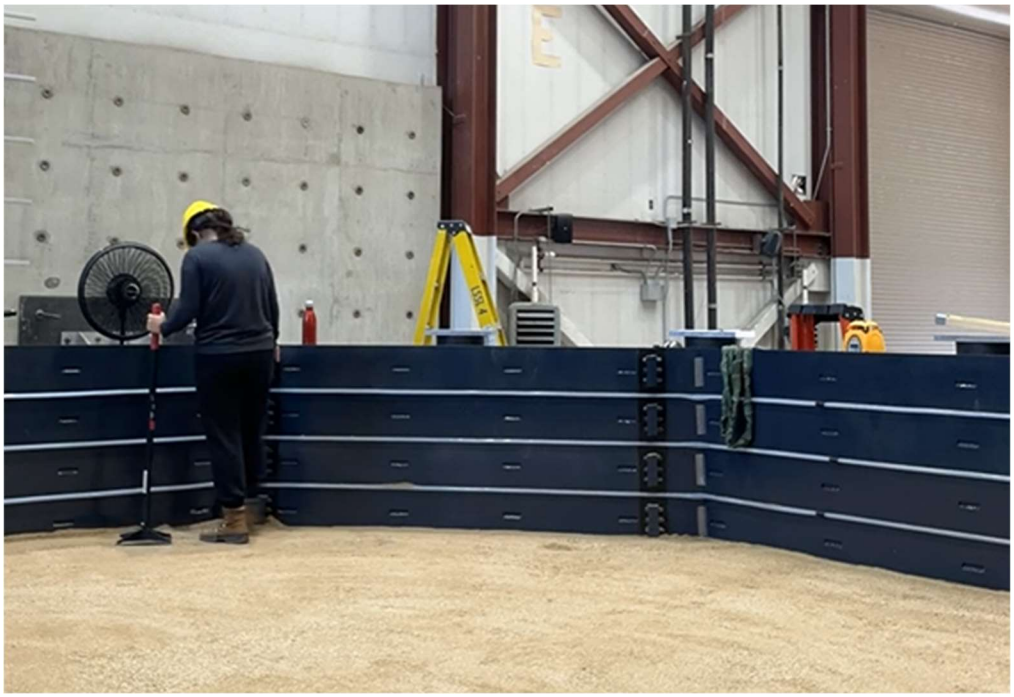

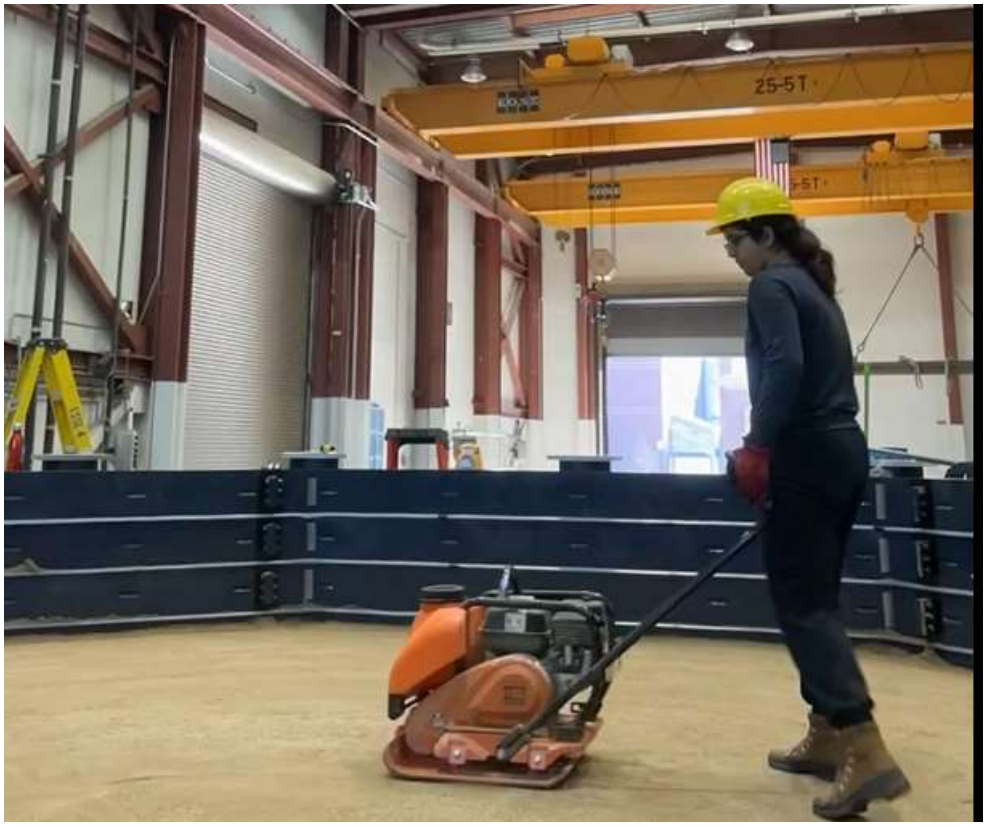
25-5T


25-5T

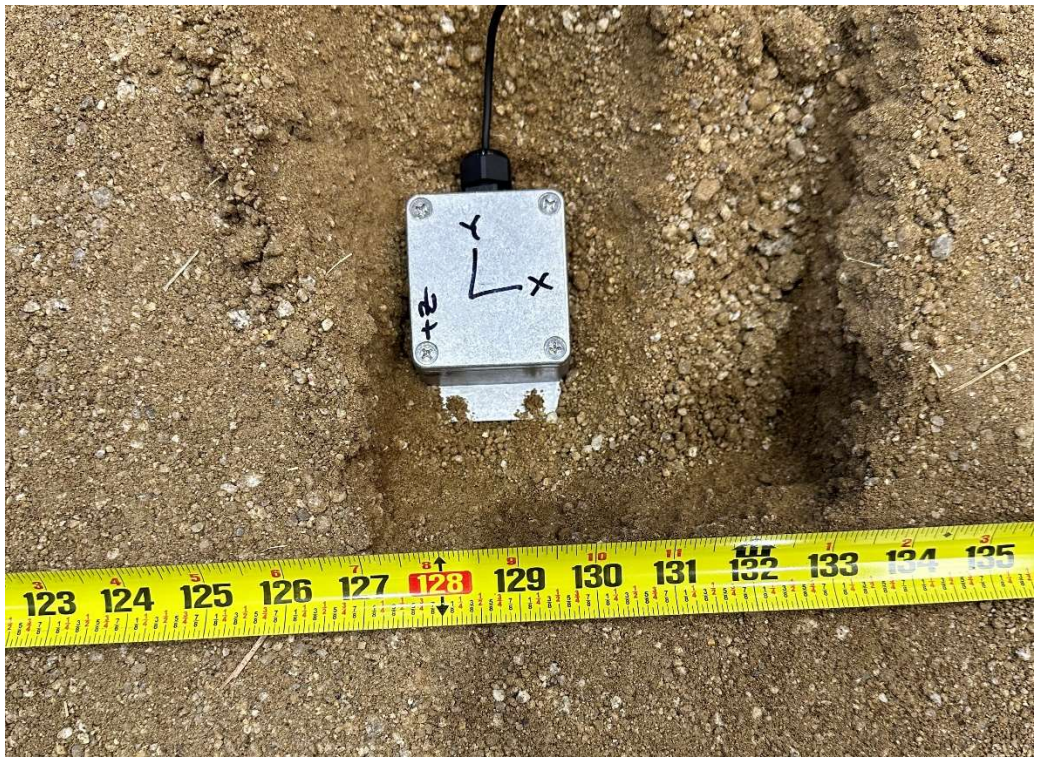
Y
Lx
+2
123
124
125
126
127
128
129
130
131
132
133
134
135

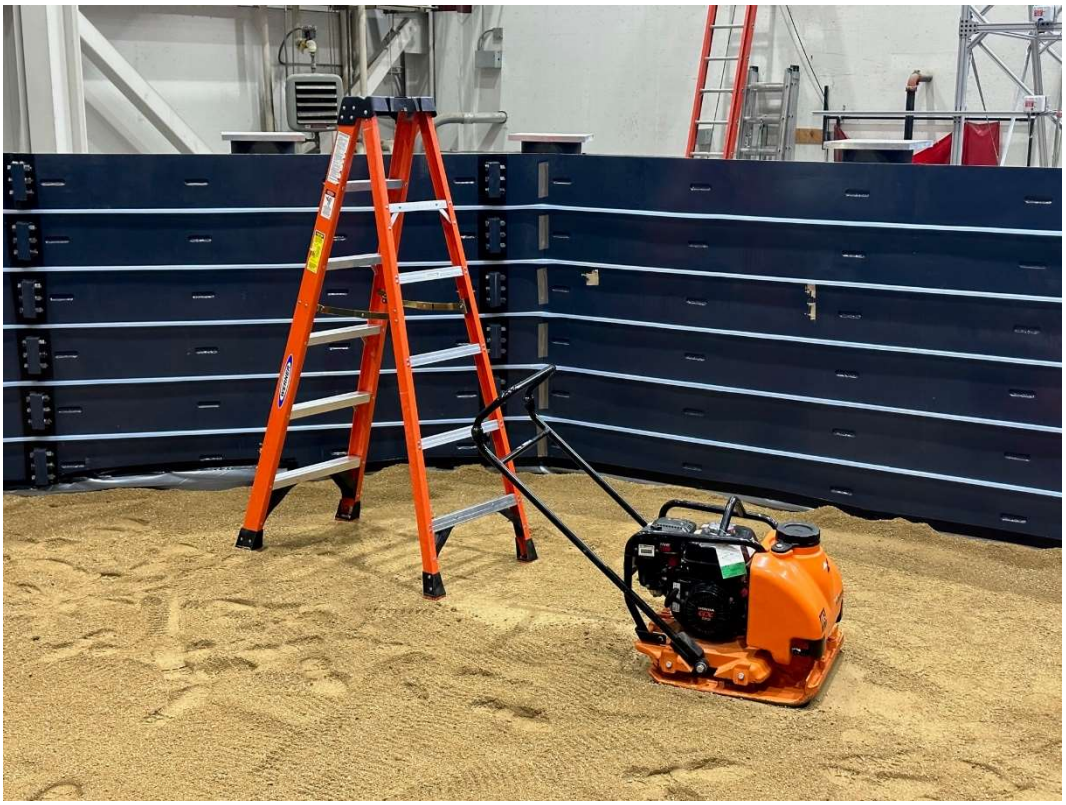


D-68
D-80

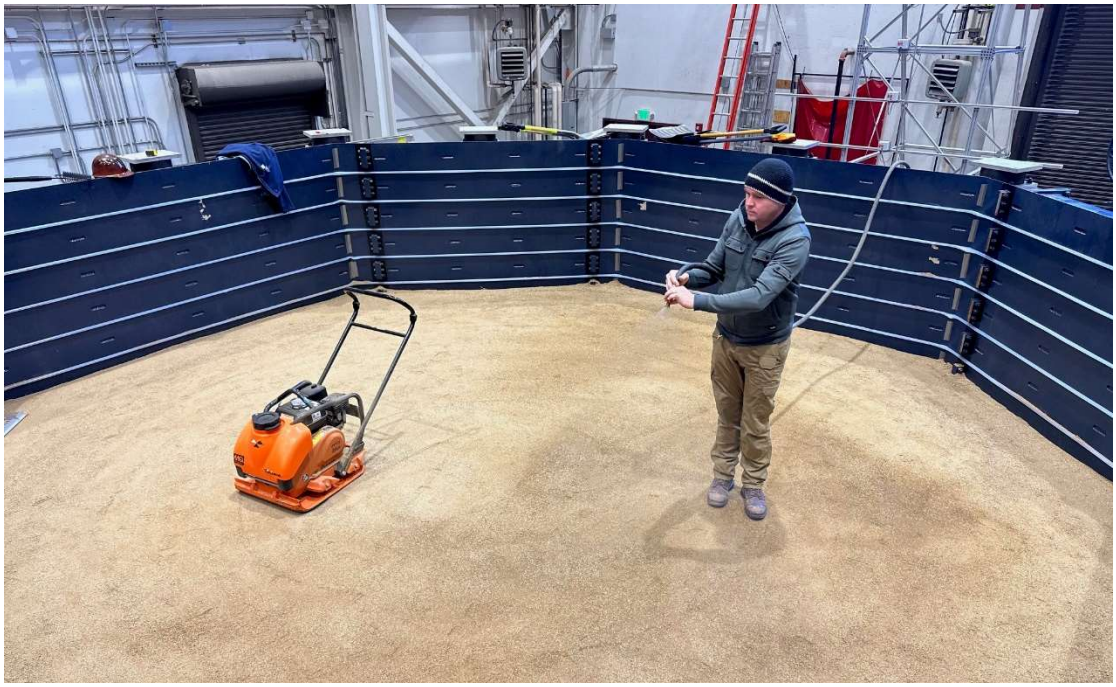


25-FT


BERKELEY LAB
N
E

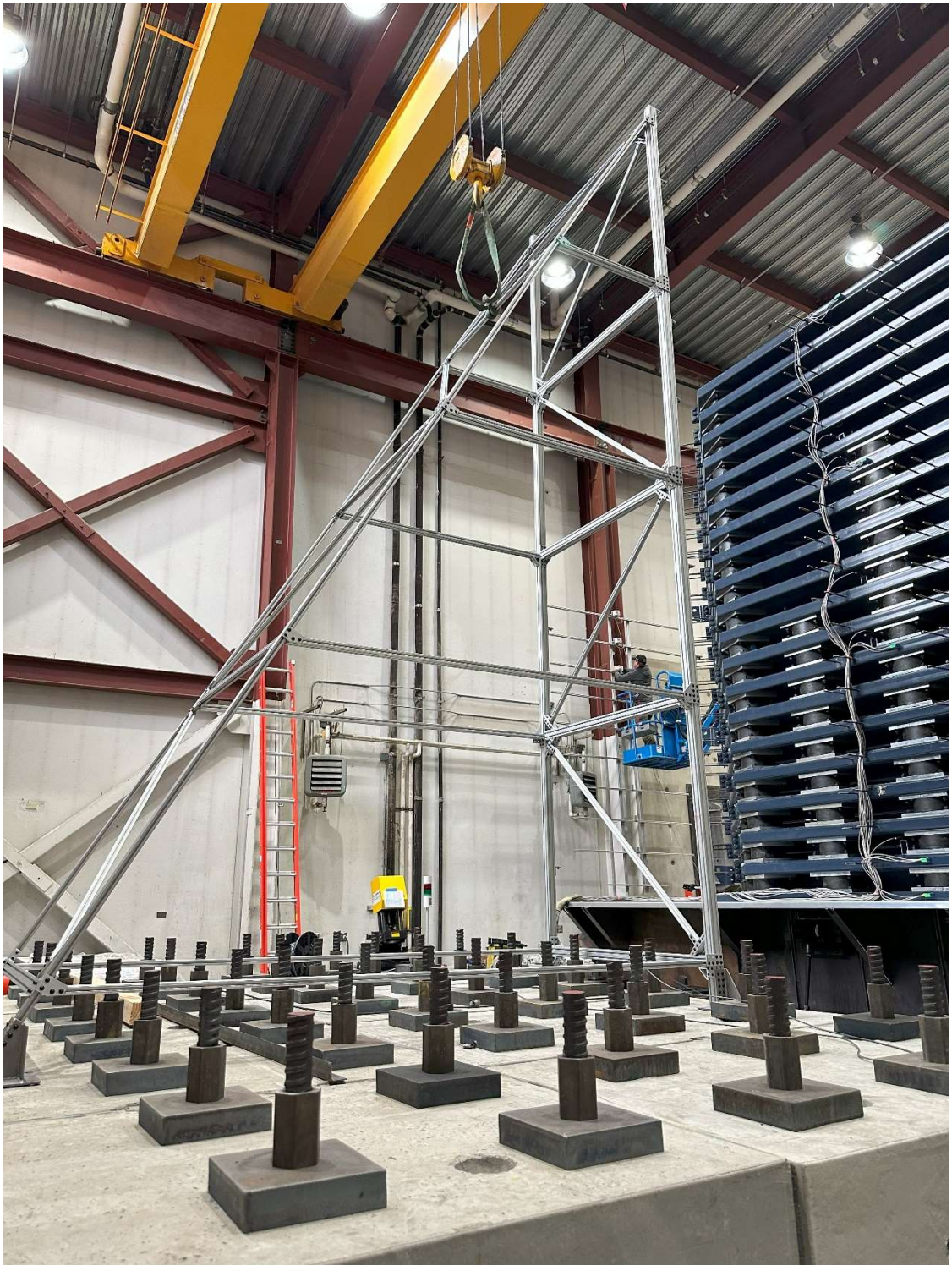


UniMeasure, Inc.
Corvallis, Oregon, U.S.A.
MODEL: PA-60
SERIAL NO.: 42120057
SENSITIVITY: 16.2635 mV/inch/V
CAUTION
DO NOT LET CABLE
SNAP BACK.
THIS MAY DAMAGE
SP60-16

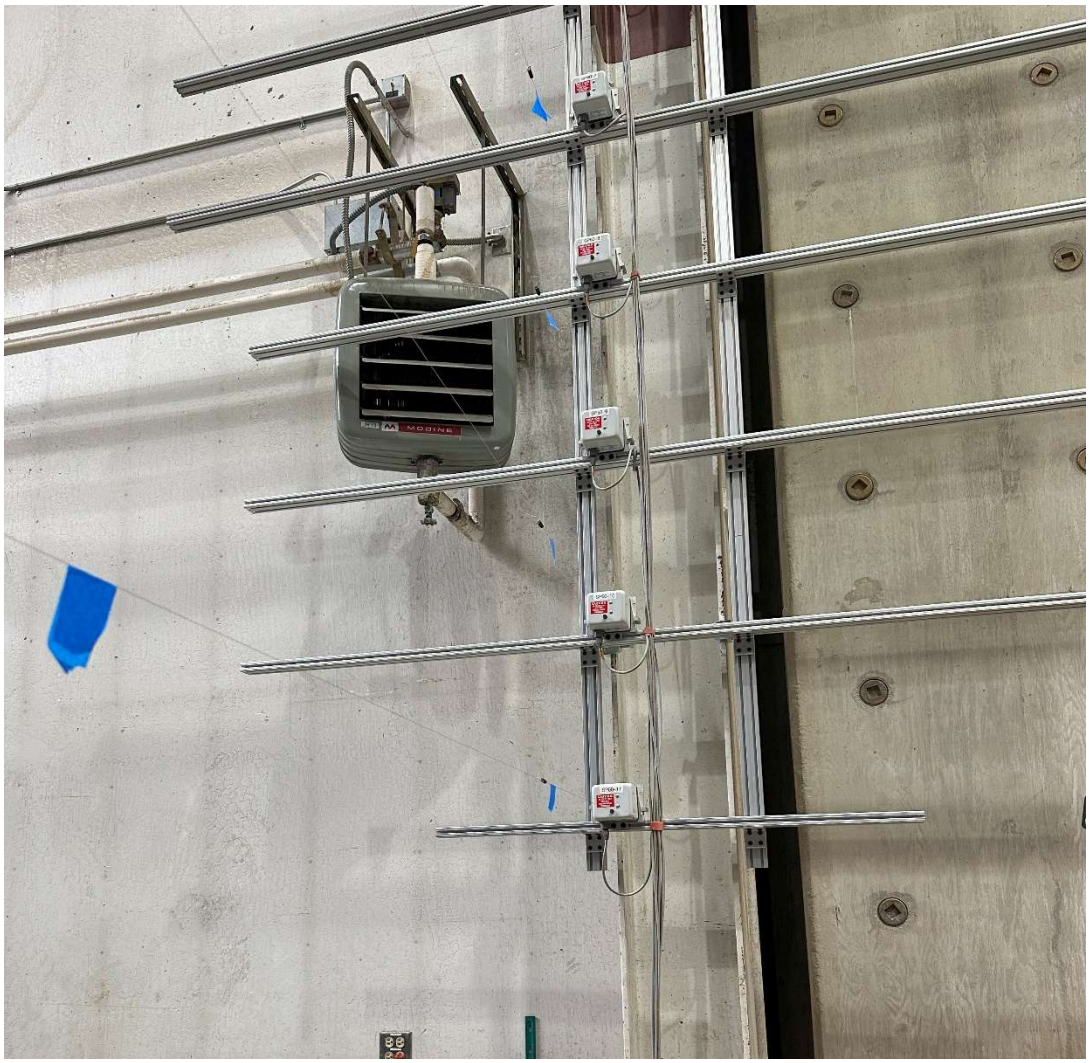

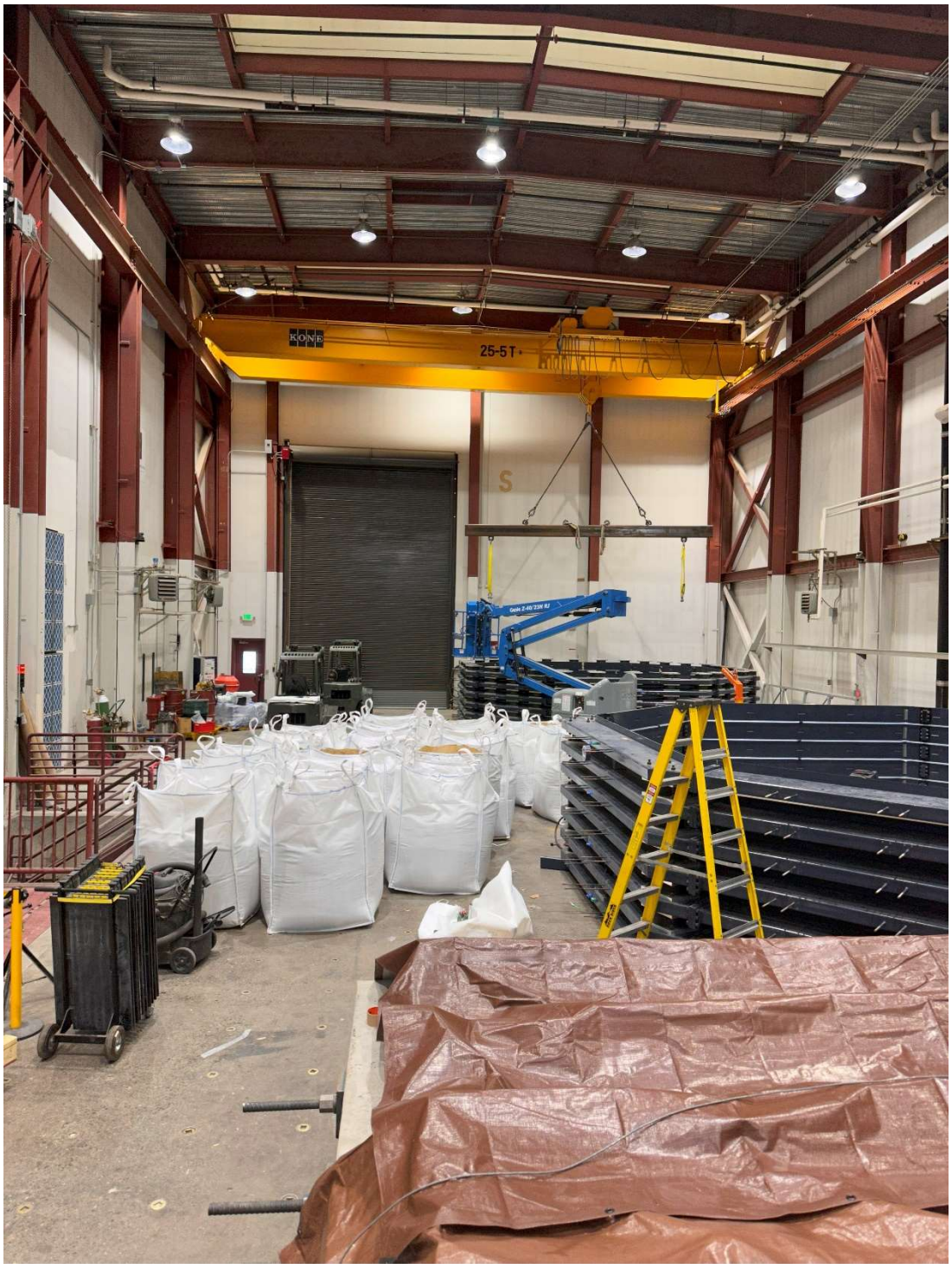
KONE
25-5T

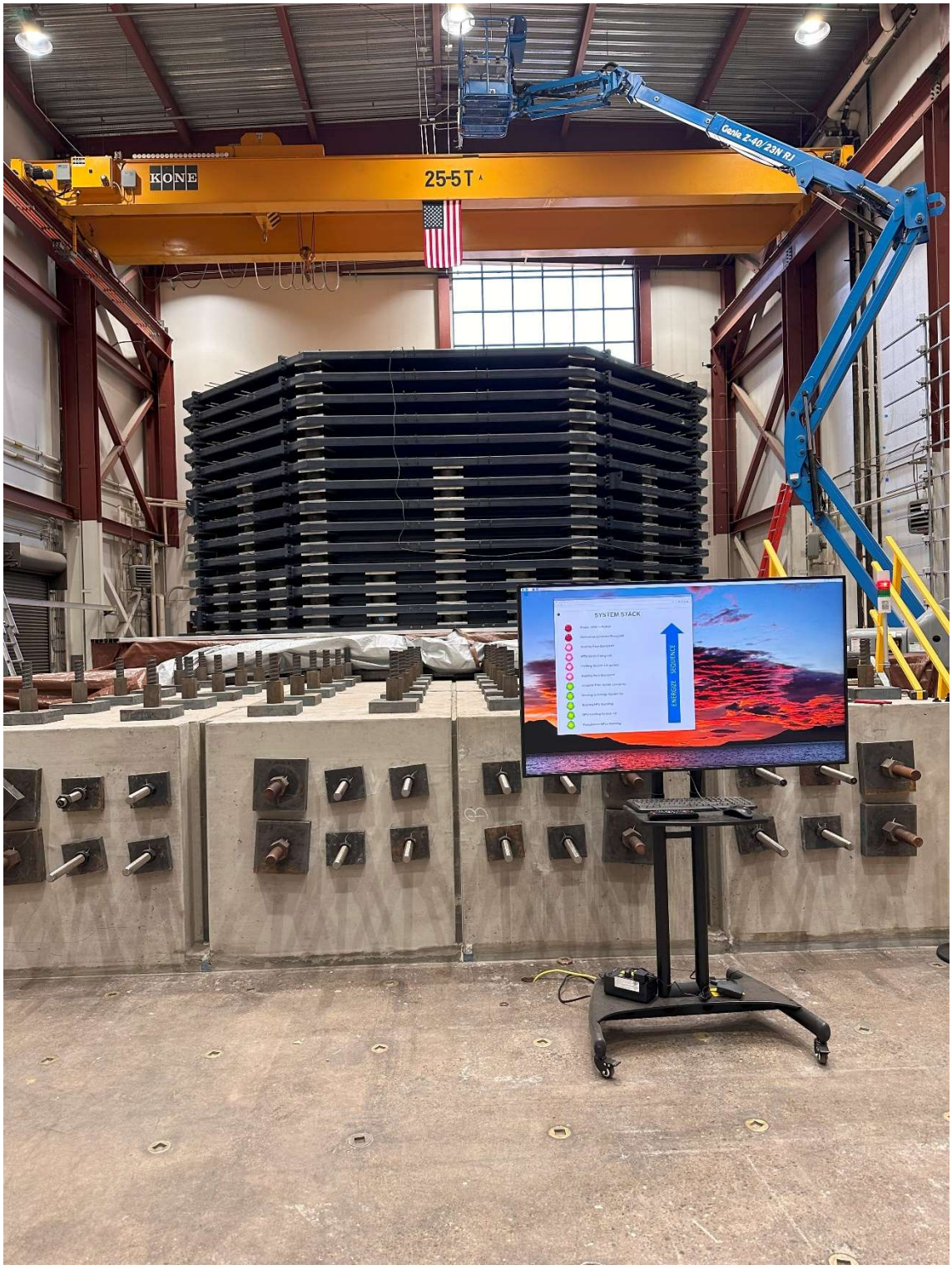
KONE
25-5T
Genie Z-40/23N RJ
SYSTEM STACK